Positional cloning and functional analysis of the resistance genes to *Bombyx mori* densoviruses

(カイコ濃核病ウイルスに対する抵抗性遺伝子の単離と機能解析)

伊藤克彦

December 19, 2008

PhD thesis

Positional cloning and functional analysis of the resistance genes to *Bombyx mori* densoviruses

Katsuhiko Ito

Supervisor: Toru Shimada

Laboratory of Insect Genetics and Biosciences,

Department of Agricultural and Environmental Biology,

Graduate School of Agricultural and Life Sciences,

University of Tokyo

Contents

General Introduction

The family of Parvoviridae

The family of Parvoviridae is characterized by a number of morphological and physicochemical properties as well as distinct features of genome organization and replication, and is taxonomically organized into two subfamilies, Densovirinae and Parvovirinae (Table 0.1). Viruses assigned to the Densovirinae infect invertebrate, whilst the Parvovirinae infect vertebrate. Viruses are small icosahedral, no-enveloped particles of 12-26 nm in diameter and their genomes consist of a 4.0-6.5 kb-long single-stranded linear DNA equimolecularly encapsidated as plus and minus strands in separate virions.

The Parvovirinae is further subdivided into five genera designated Amdovirus, Bocavirus, Dependovirus, Erythrovirus, and Parvovirus. Many viruses have been discovered from the vertebrate such as human, dog, cat, and mink (Table 0.1). Especially, human parvovirus B19, which is a member of the *Erythrovirus* genus, is a well-known and most characterized virus since this virus causes a mild childhood rash, Erythema infectisum (Kaufmann et al., 2004).

On the other hand, the Densovirinae is subdivided into four genera designated Brevidensovirus, Densovirus, Iteravirus, and Pefudensovirus. Many viruses have been identified from diverse insect groups such as *Bombyx mori*, *Junonia coenia* and *Galleria mellonella* in Lepidoptera, *Aedes aegypti* in Diptera and *Periplaneta fuliginosa* in Blattera as well as in crustaceans such as lobster and crab (Bergoin and Tejissen, 2000) (Table 0.1).

Table 0.1 Distribution of Parvoviridae

Parvovirinae	Densovirinae
Amdovirus	Brevidensovirus
Aleutian mink disease virus	*Aedes aegypti* densovirus
Bocavirus	*Aedes albopictus* densovirus
Bovine parvovirus	(*Aedes pseudoscutellaris* densovirus)
Canine minute virus	(*Penaeus stylirostris* densovirus)
Dependovirus	(*Simulium vittatum* densovirus)
Adeno-associated virus1	Densovirus
Adeno-associated virus2	*Galleria mellonella* densovirus
Adeno-associated virus3	*Junonia coenia* densovirus
Adeno-associated virus4	(*Diatraea saccharalis* densovirus)
Adeno-associated virus5	(*Mythimna loreyi* densovirus)
Avian adeno-associated virus	(*Pseudoplusia includens* densovirus)
Bovine adeno-associated virus	(*Toxorhynchites splendens* densovirus)
Canine adeno-associated virus	Iteravirus
Duck parvovirus	*Bombyx mori* densovirus*
Equine adeno-associated virus	(*Casphalia extranea* densovirus)
Goose parvovirus	(*Sibine fusca* densovirus)
Ovine adeno-associated virus	Pefudensovirus
Adeno-associated virus 7	*Periplaneta fuliginosa* densovirus
Adeno-associated virus 8	
Bovine parvovirus 2	unclassified Densovirinae
Erythrovirus	*Acheta domestica* densovirus
Human parvovirus B19	*Blattella germanica* densovirus
Pig-tailed macaque parvovirus	*Culex pipiens* densovirus
Rhesus macaque parvovirus	*Euxoa auxiliaris* densovirus
Simian parvovirus	*Leucorrhinia dubia* densovirus
(Bovine parvovirus type 3)	*Lymantria dispar* densovirus
(Chipmunk parvovirus)	*Myzus persicae* densovirus
Parvovirus	*Pieris rapae* densovirus
Chicken parvovirus	*Planococcus citri* densovirus
Feline panleukopenia virus	
HB parvovirus	
H-1 parvovirus	
Kilham rat virus	
Lapine parvovirus	
LuIII virus	
Minute virus of mice	
Mouse parvovirus 1	
Porcine parvovirus	
RT parvovirus	
Tumor virus X	
(Hamster parvovirus)	
(Rat minute virus 1)	
(Rat parvovirus 1)	

reference: Virus Taxonomy 8th report (2005)

Viruses shown in parentheses are tentative species in each genus.

*BmDNV-1

BmDNV-2 and BmDNV-Z were recently excluded from the family Parvoviridae.

Infection mechanisms of parvovirus

Infection of parvovirus initiates through capsid-mediated binding to one or more glycosylated receptor molecule on the cell surface and is followed by virion uptake into the cell via receptor-mediated endocytosis. Transfer across the delimiting lipid bilayer of the entry vesicle into the cytoplasm is then affected by a capsid-borne phospholipase, and this followed by delivery to, and entry into the nucleus, where the viral genome is finally released from its protective shell. Thus, parvovirus genomes remain associated with their intact capsids throughout the entire entry process, and possibly even in primary viral transcription complexes, so that host cell-specific interactions with the viral particle could potentially impinge at multiple stages during the initiation of infection.

Rather than interacting with a single cell surface receptor, many virus families employ two more-or-less separate classes of molecule: “attachment” receptors, or coreceptors, which simply accumulate virus in the vicinity of the cell surface; and infectious-entry receptors, which critically mediate genome transfer into the cell cytoplasm. Some members of the Parvovirinae are known to bind to a number of different cell surface molecules in ways that potentiate infection, although the extent to which they rely on multiple interactions appears to vary from species to species, and within a species from host cell to host cell, so that few general rules are apparent.

Human parvovirus B19 is a well-known virus that causes a mild childhood rash, Erythema infectisum (Kaufmann et al., 2004). B19 is thought to exclusively infect human, and shows a pronounced tropism for erythroid precursors and megakaryocytes (Broliden et al., 2006; Sundin et al., 2008). The virus is very stable and often survives in blood products despite standard procedures for viral elimination (Solheim et al., 2000).

B19 uses at least three cellular receptors for cell attachment and entry. The erythroid P antigen (globside) was known as a receptor (Brown et al., 1993). In addition, the α5β1 integrin (fibronectin) and the Ku80 autoantigen have been described as B19 coreceptors (Weigel-Kelley et al., 2003; Munakata et al., 2005). On the other hand, canine parvovirus (CPV) and feline panleukopenia virus (FPV) are also reported about their specific infection mechanisms.

Host range of densoviruses

Histopathological and pathobiological studies showed that the host- and tissue-specificities and infection mechanisms vary considerably among densoviruses (Kawase and Kurstak, 1991; Tijissen and Bergoin, 1995; Afanasiev and Carlson, 2000). *Galleria mellonella* densovirus (GmDNV), *Casphalia extranea* DNV (CeDNV) and *Acheta domestica* DNV (AdDNV) have a host range apparently restricted to their original host (Fediere, 2000). In contrast, other DNVs, also isolated from Lepidoptera, have a broader host range. *Mythimna loreyi* DNV (MlDNV) is infectious for many other lepidopterans, *Chilo agamemnon*, *G. mellonella*, *Ostrinia nubilalis*, *Pectinophora gossypiella*, *Sesamia cretica*, and *Spodoptera littoralis* (Fediere, 2000). According to their sequences and genome organization, MlDNV is very closely related to GmDNV (Fediere, 2000). The close relationship is interesting since their tropism differs greatly, GmDNV being monospecific on its host, whereas MlDNV is polyspecific and infects a large number of Lepidoptera.

Utilization of densoviruses

Mosquito densoviruses have features that make them attractive for use in integrated vector-borne disease control programs. They are relatively stable in the environment. They are exclusively targeted to mosquitoes and have the potential to spread and persist in mosquito populations by normal infection and replication mechanisms. The use of densoviruses in the fight against vector-borne disease could follow either of two potential strategies. The more conventional strategy is use of densovirus as a microbial pesticide for biological control of mosquitoes. *Aedes aegypti* DNV (AeDNV) infection affects all lifestages of *Aedes aegypti* and significantly shortens the adult lifespan to the point that the virus has the potential to significantly modify the age structure of adult mosquito populations. This in turn should significantly reduce the vectorial capacity of the population (Suchman et al., 2006). The second strategy is to develop densoviruses as transducing vectors (Afanasiev and Carlson, 2000; Carlson et al., 2000). Constructs to induce interference to arboviral infection could be introduced into mosquitoes by transduction, for "immunization" or reduction of vectorial capacity for arboviruses.

***Bombyx mori* densovirus**

Bombyx mori densovirus (BmDNV) is a pathogen of flacherie disease in the silkworm. BmDNVs multiply only in the nuclei of the columnar cells of the larval midgut epithelium (Seki and Iwashita 1983). To date, three isolates of BmDNVs have been reported: BmDNV-1 (Ina isolate), BmDNV-2 (Saku isolate and Yamanashi isolate), and BmDNV-Z (Zhenjiang isolate) (Tijssen and Bergoin, 1995). BmDNVs are classified into two major types, type I and type II, based on their genomic characteristics. The genome of BmDNV type I, BmDNV-1, contains single-stranded complementary DNA molecules that are about 5 kb in length (Bando et al., 1990). In contrast, BmDNV type II possesses a split genome comprising two types of single-stranded linear DNA molecules. BmDNVs of this type include BmDNV-2 (Yamanashi isolate) and BmDNV-Z (Zhenjiang isolate) that contains two ssDNA molecules, which are 6.0 and 6.5 kb in length (Bando et al., 1992; Bando et al., 1995; Wang et al., 2007). BmDNV type I is shown to possess higher pathogenicity to the silkworm than type II (Watanabe, 2002) (Table 0.2).

According to the previous classification, BmDNV-1, -2, and -Z had been assigned into Densovirinae of the Parvoviridae. BmDNV-1 was classified as a genus *Iteravirus*, while BmDNV-2 and -Z were classified into a genus *Bidensovirus*. However, BmDNV-2 and -Z were recently excluded from the family Parvoviridae because of their genome organization and presence of a DNA polymerase motif in their own genomes (Fauquet et al., 2005).

Table 0.2 Distribution of BmDNV

Character	BmDNV-1	BmDNV-2	BmDNV-Z
Virion size	20 nm	24 nm	24 nm
Genome Topology	linear	linear	linear
Genome Molecule	ssDNA	ssDNA	ssDNA
Genome size	5.0 kb	6.0 kb, 6.5 kb	6.0 kb, 6.5 kb
Target tissues	midgut columner cel	midgut columner cel	midgut columner cell cup shaped cells*
Number of ORF	4	6	7

*BmDNV-Z can infect the cup shaped cells of midgut epithelium during the late stage of infection.

Histopathological features of BmDNVs

The silkworm larvae infected per os with the BmDNVs usually die after seven days showing body flaccidity as a major sign. The alimental canal of the diseased larvae shows pale yellow with little internal content. Although this symptom is similar to that of the infectious flacherie virus (IFV), but the histopathological features differ between the two viruses (Shimizu, 1975). All BmDNVs multiply only in the muclei of columnar cells of the midgut epithelium, and no pathological changes are observed in goblet cells of the midgut or other tissues.

Histopathological studies on the midgut epithelium of the silkworm infected with BmDNV-1, -2, and -Z showed that nuclei of the columnar cells hypertrophied and stained markedly with the Feulgen reaction or methyl green (Watanabe et al., 1976; Seki and Iwashita, 1983; Wang et al., 2007). The degenerated columnar cells were liberated into midgut lumen (Fig. 0.1).

BmDNV-2 and -Z have bipartite genomes and are classified into the parvo-like viruses, but their virulence and the symptoms of infection are different from each other. BmDNV-2 almost exclusively infects the columnar cells of midgut epithelium, while BmDNV-Z can infect the columnar cells of midgut epithelium during the early stage of infection and is able to infect the goblet cells of midgut epithelium during the late stage of infection (Wang et al., 2007).

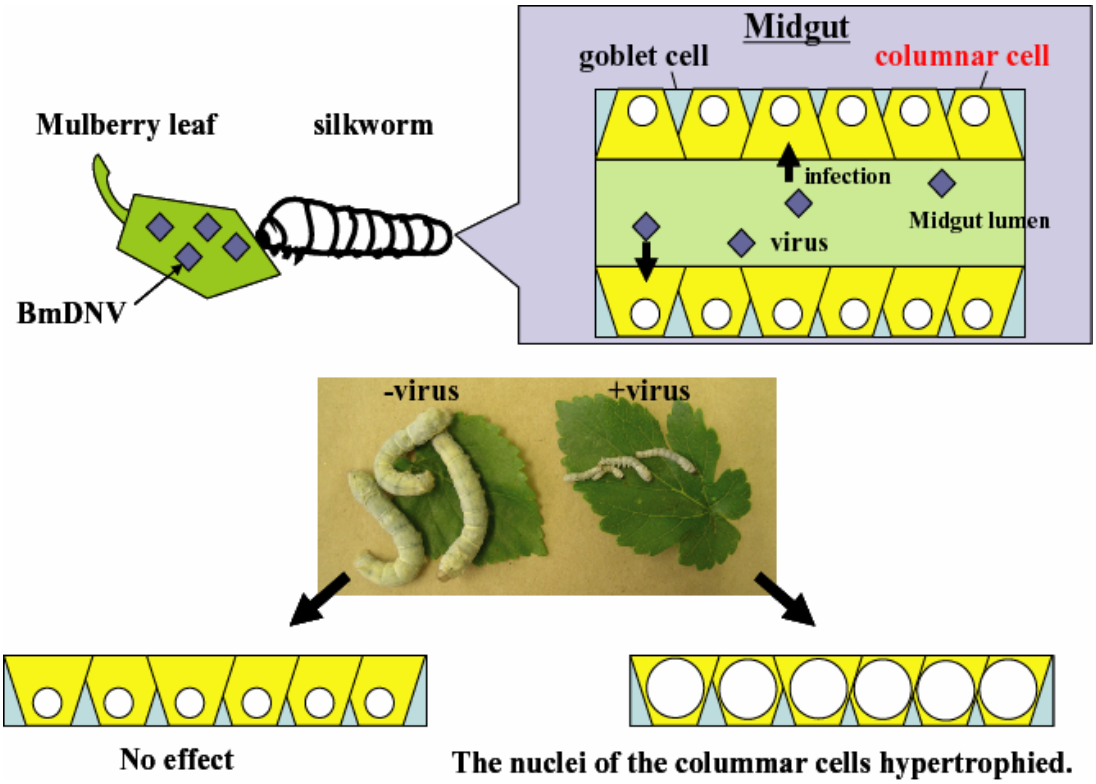

Figure 0.1 Infections of *B. mori* larvae with BmDNVs

The silkworm larvae infected per os with the BmDNVs usually die after seven days showing body flaccidity as a major sign. BmDNV infects the columnar cells of midgut epithelium, and they multiply only in the nuclei of columnar cells of the midgut epithelium.

Resistance genes to BmDNVs

Certain silkworm strains show high susceptiblity, while other strains are nonsusceptible to BmDNVs even though they are fed a high concentration of virus inocula (Watanabe and Maeda, 1978, 1981; Seki, 1984). Nonsusceptibility to BmDNV-1 is controlled by two *B. mori* genes, *Nid-1* (Non-infectious to densonucleosis virus) and *nsd-1* (non-susceptibility to densonucleosis virus type-1) (Watanabe and Maeda, 1981; Eguchi et al., 2007). On the other hand, BmDNV-2 and BmDNV-Z are controlled by *nsd-2* (nonsusceptibility to DNV-2) and *nsd-Z* (non-susceptibility to densonucleosis virus type-1), respectively (Ogoyi et al., 2003; Qin et al., 1996). It has been shown that these genes are located on different chromosomes (Abe et al., 1987). *Nid-1*, *nsd-1*, and *nsd-2* have been mapped at the position 31.1 cM on chromosome 17 (Eguchi et al., 2007), at 8.3 cM on chromosome 21 (Eguchi et al., 1991), and at 24.5 cM on chromosome 17, respectively (Ogoyi et al., 2003). In addition, *nsd-Z* was mapped on chromosome 15 (Qin et al., 1996). Although the mutations have been mapped with phenotypic and DNA markers, their responsible genes have not been identified (Fig. 0.2 and Table 0.2).

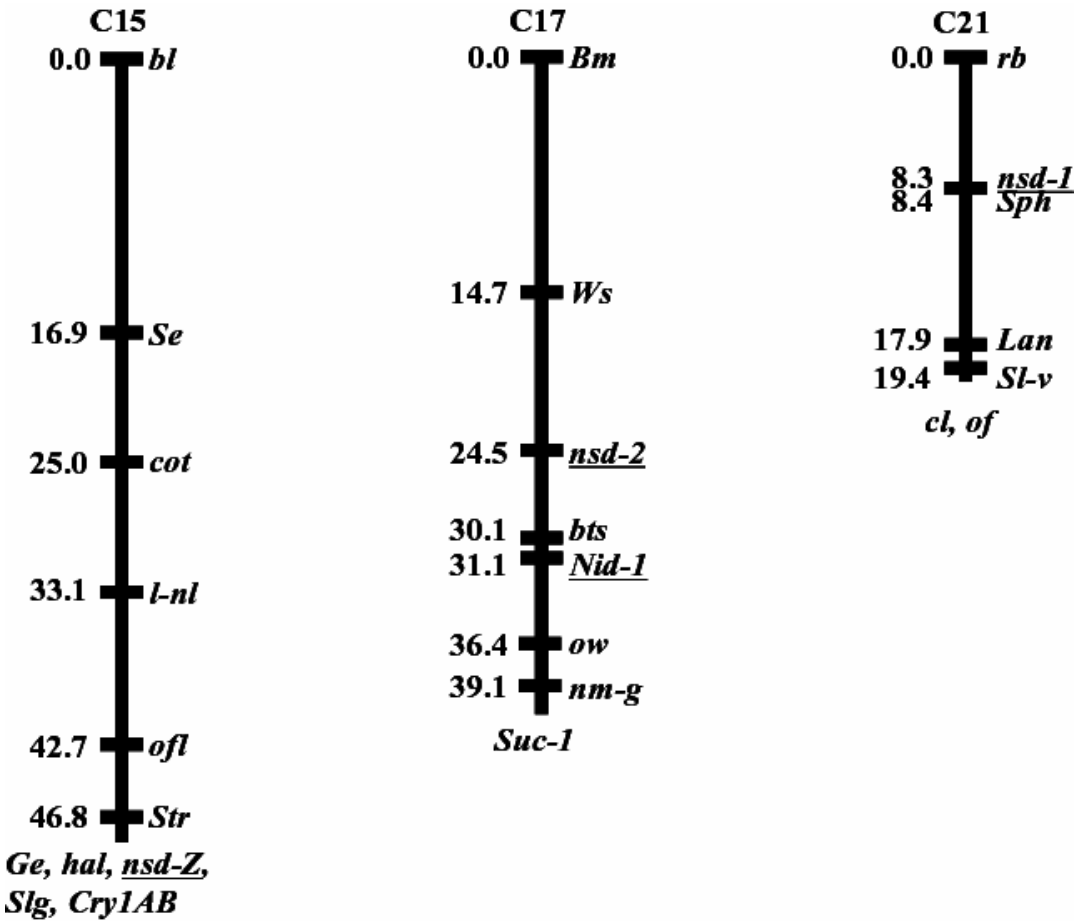

Figure 0.2 Chromosomal locations of *B. mori* resistance genes to BmDNVs

The distance is shown in centiMorgan units (cM). *Nid-1, nsd-1, nsd-2,* and *nsd-Z* has been mapped at the position 31.1 cM on chromosome 17, 8.3 cM on chromosome 21, 24.5 cM on chromosome 17, and on chromosome 15, respectively.

Bombyx mori genome information

In *B. mori*, more than 400 Mendelian mutations have been described (Doira, 1992; Goldsmith, 1995). An important potential resources of genetic variation are thousands of geographic races including practical breeding stocks, maintained in many countries. The silkworms are optimized by controlled breeding and selection for economically important quantitative traits such as growth rate, cocoon size, silk filament quality, and disease resistance (Goldsmith et al., 2005). On the other hand, many mutations related to their coloring, shape, and pattern of throughout all developmental stages are also maintained. However, the genes responsible for the mutants are largely unknown.

Recently, the *B. mori* genomic information has been updated. In 2004, Japanese and Chinese groups independently published their *B. mori* whole genome shotgun (WGS) sequence data (Mita et al., 2004; Xia et al., 2004). In 2008, a newly assembled sequence database (Build2) was constructed by integrating both WGS data. In addition, the SNP linkage map of *B. mori* has been developed (Yamamoto et al., 2006; Yamamoto et al., 2008). Combined with the classical genetic resources, these information and molecular markers will be powerful tools for map-based cloning of genes of an industrial and agricultural interest.

Aims of the present study

The aim of this study was to explore and clarify the mechanism of absolute resistance of *B. mori* to BmDNVs. As the first approach, I aimed isolation and characterization of two mutant genes *nsd-1* and *nsd-2*, which control the infectivity of BmDNV-1 and BmDNV-2, respectively, because these genes appeared to be the key factors in BmDNV infection.

To this end, I performed the positional cloning and functional analysis of the *nsd-2* (Chapter 1) and *nsd-1* (Chapter 2).

In General Discussion, I argued the molecular interactions between the isolated resistance genes and BmDNVs.

Chapter 1

Deletion of a gene encoding an amino acid transporter in the midgut membrane causes resistance to BmDNV-2

1.1 Introduction

Bombyx mori densovirus (BmDNV) is characterized by a very narrow host range and tissue specificity. Four unlinked mutations, *nsd-1* (Watanabe and Maeda, 1981), *Nid-1* (Eguchi et al., 2007), *nsd-2* (Ogoyi et al., 2003) and *nsd-Z* (Qin and Yi, 1996), which were originally discovered in different *Bombyx* strains, control nonsusceptibility to infection by two distinctly different types of virus, BmDNV-1, and -2 (or Z). Previously, both BmDNV-1 and -2 had been assigned to Densovirinae in Parvoviridae. BmDNV-2 was recently excluded from the family Parvoviridae, because, in contrast to the accepted characters for the group, its genome is split into two molecules and contains its own DNA polymerase motif (Tattersall et al., 2005).

Although the resistance genes have been mapped with phenotypic or DNA markers, they have not been isolated yet (Goldsmith et al., 2005). The identification of these genes will provide important information for understanding the host- and tissue-specificity and infection mechanisms of the corresponding densoviruses. As *nsd-2* has been well-mapped with flanking DNA markers (Ogoyi et al., 2003) and *B. mori* genome information have markedly accumulated, I undertook map-based cloning of this gene.

1.2 Materials and Methods

1.2.1 Silkworm strains and viral inoculation

Strains resistant to BmDNV-2 were J124, J150 and No. 902 (National Institute of Agrobiological Sciences, NIAS origin); susceptible strains were, C124, J203, No. 908 (NIAS), C108T, p50T (The University of Tokyo), and B (Hokkaido University). *Bombyx mandarina* (collected in Tsukuba City) was also used as a closely related susceptible species. For linkage analysis, single-pair backcrosses (BC_1) between J150 females and F_1 males (J150 female × No. 908 males) were used.

To obtain stable binary GAL4/UAS transgenic strains, the activator, enhancer trap strain of A3GAL4 (Fig. 1.1), 52-2-1 was chosen and was able to direct transgene transcription in the midgut. The activator strain was made by the cross (52-2-1 × J124) × J124 to replace the $+^{nsd\text{-}2}$ gene of 52-2-1 with the homozygous *nsd-2* gene of J124, because 52-2-1 was susceptible. For the effector strains, the effector construct (Fig. 1.1) and the transposase-carrying helper plasmid, *pHA3PIG* (Tamura et al., 2000), were injected into homozygous *nsd-2* J124 preblastoderm embryos at a concentration of 0.2 mg/ml. After sibling selection with the marker, EGFP, the G_1 moths of the UAS line were crossed with the BC_1 moths of the GAL4 line to generate $+^{nsd\text{-}2}$-overexpressing GAL4/UAS lines. The progeny of this cross showed four different phenotypes in terms of eye color: both DsRed2- and EGFP-positive, GAL4/UAS line, [GAL4(+), UAS(+)]; only DsRed2-positive, GAL4 line, [GAL4(+), UAS(–)]; only EGFP-positive, UAS line, [GAL4(–), UAS(+)]; and neither DsRed2- nor EGFP-positive, wild type, [GAL4(–), UAS(–)].

The transgenic and wild-type strains and the related species, *B. mandarina,* were reared at 25°C. A BmDNV-2 inoculum was prepared, and larvae were treated as

described previously (Abe et al., 2000). The newly hatched first instar or the newly ecdysed fourth instar larvae were fed mulberry leaves smeared with BmDNV-2 suspension at 10^{-2} diluted supernatant of midgut homogenate from BmDNV-2-infected larvae.

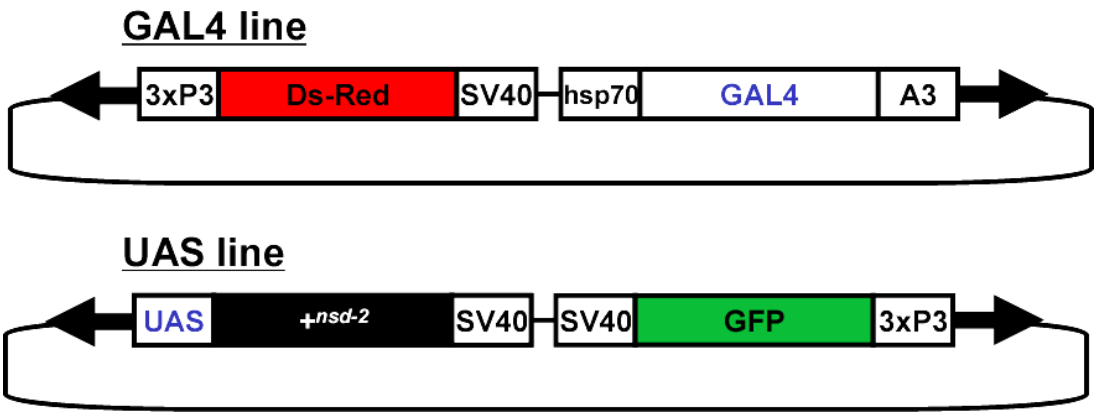

Figure 1.1 Plasmid constructs for transgenic silkworm

Upper figure indicates the activator construct of *pBacMCS*[*BmA3-GAL4-3xP3-DsRed2*]. It contains a full ORF of yeast transcriptional factor GAL4 under the control of the BmA3 promoter and the marker gene, DsRed2, under the control of the 3xP3 promoter. Lower figure indicates the effector construct of *pBacMCS*[*UAS-*$+^{nsd\text{-}2}$*(No. 908)-SV40-3xP3-EGFP*]. It contains a DNA-binding motif, UAS, for GAL4, linked to the ORF of the targeted gene, $+^{nsd\text{-}2}$, and the marker gene, EGFP, under the control of the 3xP3 promoter. Arrows indicate *piggyBac* inverted terminal repeats.

1.2.2 Chromosome walking and positional cloning

Chromosome walking was performed by BAC high density replica filter hybridization (Koike et al., 2003) with PCR-amplified probes designed with sequences derived from BAC clone ends, EST clones, and genome shotgun data. The new primers were designed with the end sequences of screened BAC clones which were most distal in aligned BAC clones. This approach was repeated to extend the BAC contig. For positional cloning, PCR, RFLP and sequencing markers were generated for each position of the walked region, and the markers which showed polymorphism between the parents were used for linkage analysis of 206 BC_1 moths selected with virus inoculation from about 500 individuals.

1.2.3 Isolation of genomic DNA and total RNA

Genomic DNA was isolated from whole bodies of individual moths or fifth instar larvae as described (Ogoyi et al., 2003), modified by homogenization with stainless steel beads instead of mortar and pestle with liquid nitrogen. Genomic DNA of individual transgenic silkworms was isolated from a small portion of the body using DNAzol (Invitrogen) according to the manufacturer's protocol. Day 1 fourth instar larvae were used for the isolation of total RNA from individual tissues, including silk gland, foregut, midgut, hindgut, Malpighian tubule, fat body, testis plus ovary, and central nervous system. In the isolation of total RNA from individuals of different stages, eggs of day 0, 4, and 10, whole body from day 0 of first instar to fourth instar larvae, midgut from day 1, 2, 3 and 4 of fourth instar, day 0, 2, 4 and 6 of fifth instar, day 0, 7 of pupae and day 0 of adults were used. Total RNA was purified with TRIzol (Invitrogen) according to the manufacturer's protocol. Full-length cDNAs were determined using a SMART RACE

cDNA Amplification Kit (Clontech) according to the manufacturer's protocol.

1.2.4 Annotation analysis

The resistant/susceptible strain-specific sequences that I found in the region narrowed by linkage analysis were subjected to analysis by using KAIKOGAAS (http://kaikogaas.dna.affrc.go.jp) for annotation and KAIKO blast (http://kaikoblast.dna.affrc.go.jp) and NCBI blast (http://www.ncbi.nlm.nih.gov/BLAST) to look for homologs and othologs.

1.2.5 Plasmid construction

The effector plasmid construction (UAS line) was generated by the following method. The susceptibility gene, $+^{nsd\text{-}2}$, was amplified by PCR from the cDNA clone using KOD-plus-DNA polymerase (TOYOBO). Both forward and reverse primers contained an *Xba*I site. The PCR product was subcloned to a pCR-Blunt II-TOPO vector (Invitrogen), and the subcloned product was digested with *Xba*I. The fragment obtained was ligated into *pBacMCS-UAS.SV40-3xP3EGFP* previously digested with *Bln*I. The PCR product and constructed plasmid, *pBacMCS-UAS-*$+^{nsd\text{-}2}$*(No. 908)-SV40-3xP3EGFP*, were confirmed by DNA sequencing.

1.3 Results

1.3.1 Chromosome walking and fine mapping of *nsd-2*

For the identification of a candidate region for *nsd-2*, chromosome walking was started from three EST markers shown to be closely linked with the mutation by RFLP mapping (Ogoyi et al., 2003) (Fig. 1.2A), then elongated up- and downstream to generate additional markers closer to *nsd-2* by BAC library screening (Koike et al., 2003). A diagram of the physical and genetic maps generated in the walk is shown in Fig. 1. A BAC contig of approximately 5 Mb was constructed that covered the up- to the downstream boundaries of the *nsd-2* linked region (Fig. 1.2B). By genetic linkage analysis using this physical map, the *nsd-2* linked region was narrowed to between the T7 end of BAC clone, 034C07, and the SP6 end of BAC clone, 001K10 (Tables 1.1 and 1.2). The region was about 400 kb in length and covered by four BAC clones, 022C09, 067M09, 021B10, and 059I11 (Fig. 1.2C).

In the comparison between resistant (J150) and susceptible (No. 908) strains using primers designed within the narrowed region, I found a critical region on the T7 end of BAC clone, 067M09. The primers constructed for the region gave no PCR products only in the resistant strain. Furthermore, it was found that the resistant strain had a deletion of about 6 kb and an insertion of 34 bp in this region. In a more comprehensive PCR survey of other resistant and susceptible strains, including *B. mandarina*, the most closely related living wild silkmoth having a putative common ancestor of *B. mori*, the long deletion and the very short insertion were common to all the resistant strains (Fig. 1.2D). The primers encompassing the long deletion gave size varieties in susceptible strains, which is explained in detail in the next section.

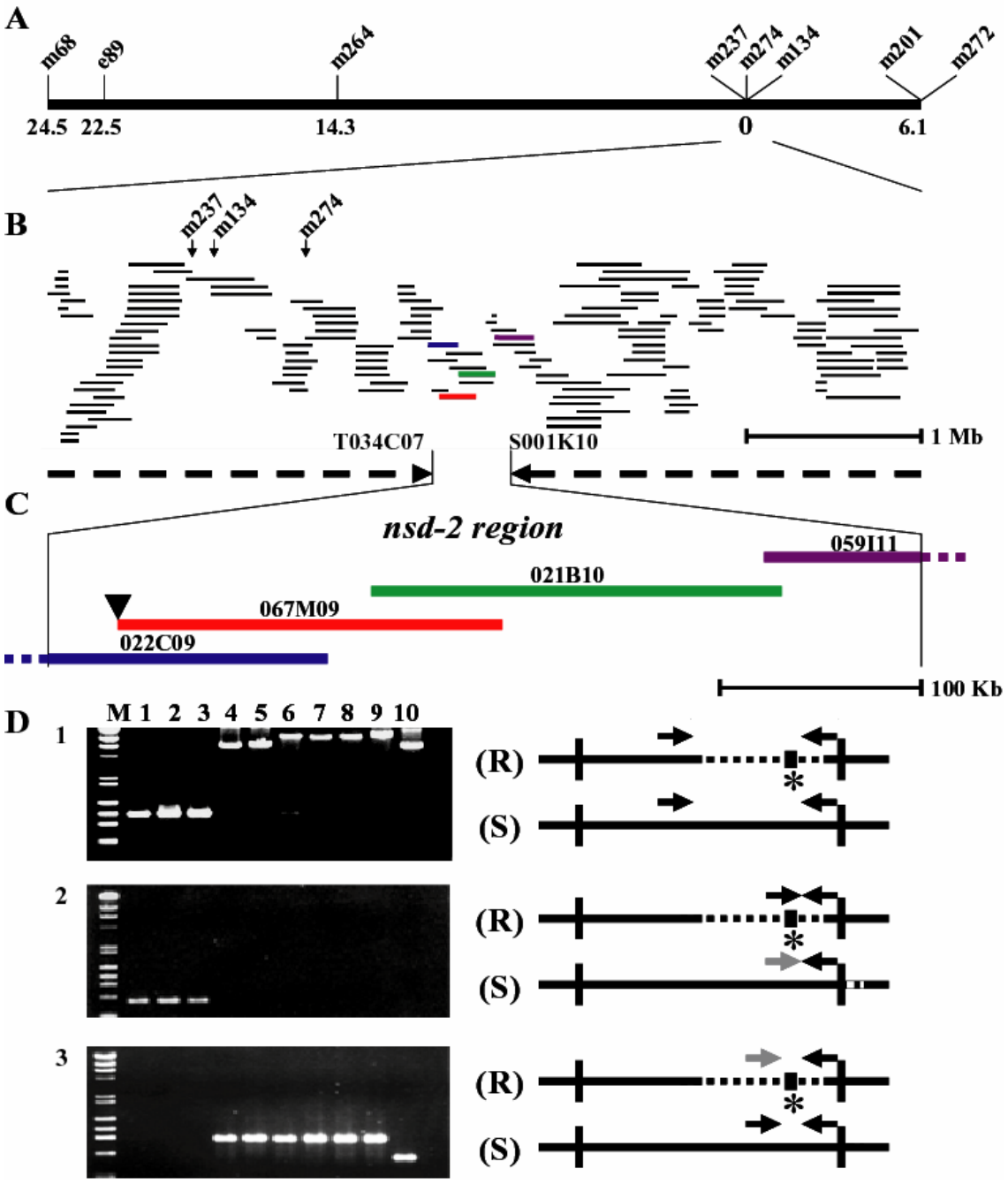
A
m68
e89
m264
m237
m274
m134
m201
m272
24.5
22.5
14.3
0
6.1
B
m237
m134
m274
T034C07
S001K10
1 Mb
C
nsd-2 region
059I11
021B10
067M09
022C09
100 Kb
D
M 1 2 3 4 5 6 7 8 9 10
1
2
3
(R)
(S)
(R)
(S)
(R)
(S)

Figure 1.2 Chromosome walking and mapping of *nsd-2*

Mapping of *nsd-2* on linkage group 17. (A) RFLP map of *nsd-2*, modified from the previous report (Ogoyi et al., 2003). EST markers are shown above the map, whereas the distance between the markers and *nsd-2* is shown in centiMorgan units (cM) below the map. EST markers m237, m274, and m134, which showed no recombination with *nsd-2* in the initial study involving 49 male informative backcross (BC_1) progeny, served as the starting point for the walk (Ogoyi et al., 2003). (B) BAC contig covering 3 EST markers. Each line shows a BAC clone. A dotted line indicates the result of linkage analysis using 206 BC_1 progeny surviving virus treatment to narrow the region linked to *nsd-2*. (C) Minimum BAC tiling path for the region closely linked to *nsd-2*. The arrowhead indicates the locus where the deletion was found specifically in resistant strain J150. (D) PCR amplification of genomic DNA from resistant and susceptible strains PCR-amplification of genomic DNA from resistant and susceptible strains at the region indicated by the arrowhead in C. Left, PCR patterns; right, the position of primer sets in the resistant strain J150(R) and the susceptible strain No. 908(S): (1) the forward and the reverse primers encompass the deletion (dotted line); (2), the forward primer includes the specific intact sequence in J150; and (3) the forward primer is within the deletion. M, λand ϕX174 DNA digested individually with *Hin*dIII and *Hae*III, and mixed as molecular markers; lane 1, J150; 2, J124; 3, No. 902; 4, No. 908; 5, J203; 6, C124; 7, B; 8, p50T; 9, C108T; 10, *B. mandarina*. 1–3, resistant; 4–10, susceptible.

Table 1.1 The primers used in this research

object	name	sequence (5' - 3' end)
linkage analysis in Table 2	32L06T-CF	TGTTCTTRCGTGGCTAGAAACKC
	32L06T-CR	TTATAATAGGTTACAAGATCGAAGAAG
	35D24SF	GGGTATATAGATTTGGATTGACGAAC
	35D24SR	TTACAAATGTAATGTAATGTTGGTCAC
	57-F	GGGATGACTGGATTGCCCTTG
	57-R	CTTTTTATTTGTATCTCGACTAGCG
	Sc14398-F	ATCAGCCGCAACTTGGGATGTTG
	Sc14398-R	GAAATCACTTTTGCGTAGCTCATAC
	34C07T-F	ATTGCTGTTTTAACCGGCTGAATAC
	34C07T-R	TTGATTGCAGTTTACAACACCAGAC
	67M09T-F	ACTGAAGCACTAGGAGGTCCGTTAAA
	67M09T-R	CAATAGTTTCAGTGATAGCCGCGAAC
	Sc337-3F	TCCCTAGATCGACCTCTTGATTCAC
	Sc337-3R	GTATTCCACCACCATCATATCCACCT
	15A12T-F	GGTATCAGGAGACTTCTGCCCATTT
	15A12T-R	AATGTGCTTTAGGGGAATCACGTTT
	22C09T-F	GCTGACCAGCTTACAATGAATAGTC
	22C09T-R	AGCTGGAAAGAAGTCAATATGAGAC
	06E02S-F	GCGAAGTAAAATGCTATACTGTTCC
	06E02S-R	CACACTTTGAAGGTGCGTGCATG
	01K10S-F	AACCAATAAGGGGTAGAGTTGAAGG
	01K10S-R	CACACACAATTTATAAACCGCAACTT
	10M15S-F	AAATGCCGTGAGATTGTCTAGTAC
	10M15S-R	CAGAGACCTCCTTGCCGGTATC
	23J20T-F	TCCGCCTTTTGTAGTCGGCTTC
	23J20T-R	CTGGAAACATGATTCCCTAGCGAC
	12E17T-F	TGGTTTGAAACACAGTTCCGTTCAC
	12E17T-R	CTATGAGCTCCACCATTGAACAG
	70B11T-F	GAGTTTAATGTTAATGCGATTCGAG
	70B11T-R	CGACTCTTGACGTAGTTGTCAAG
	14C12T-F	TAGGTAGGAAGATCCACTACGATG
	14C12T-R	TAGTAGTACCAGGGACTGTTGTTG
	58F21S-F	CTAAAAGCTAGGAACACTCGTTTAG
	58F21S-R	TGACTAGCACGGCCTGGAAATAG
	83J16S-F	AAATCCTCGCCAATAGAAATGAACG
	83J16S-R	CAGCCTTTACATTTTGCCGATACAA
detection of deletion or specific sequence of resistant strains in Figure 1.2D	1-F	TCTACGTGCTTTCATACTACGTATC
	1-R	TTCCTCACGTTTCTGAATTTCTCTTG
	2-F	TTTACGTGTTAATTTACGTAACGTTAC
	2-R	TTCCTCACGTTTCTGAATTTCTCTTG
	3-F	GGTAAGAGGTCCAACGCTGTTAAGTT
	3-R	TTCCTCACGTTTCTGAATTTCTCTTG
RT-PCR of *nsd-2* candidate in Figures 1.4	*nsd-2*-F	ACTTCCAAAGCGAATGTTGAAGCG
	nsd-2-R	ACATTTTTTAATCTACCGCTTCCTG
positive control for RT-PCR (18S RNA)	18S-F	TTGACGGAAGGGCACCACCAG
	18S-R	GCACCACCACCCACGGAATCG
plasmid construct for $+^{nsd-2}$ transgene	transgenic-F	TCTAGAATGGATTCAAATGGGATAAATGAAAAG
	transgenic-R	TCTAGACATACATTTTTTAATCTACCGCTTCC
check for the transgenic silkworm in Figure 1.7	UAS-*nsd-2* -F	AGCAACCAAGTAAATCAACTGCAAC
	UAS-*nsd-2* -R	AAAGGCAAAGGGCGATGATTGA
	DNV-2-F	GAAGATACTGTCCCAAATGA
	DNV-2-R	CCTTCAGGTTTAGCTTCTTG
	nsd-2 / $+^{nsd-2}$-F	ATGGGAAGAAAAGAAACGTGGCTG
	nsd-2 / $+^{nsd-2}$-R	TTCCTCACGTTTCTGAATTTCTCTTG

Table 1.2 Linkage analysis of BC_1 segregants

primer sets	method	150	908	F_1	BC_1*																					
					1	2	3	4	5	6	7	8	9	10	11	12	13	14	15	16	17	18	19	20	21	22	23
32L06T-CF/CR	PCR	A	B	A/B	A/B	A/B	A/B	A/B	A/B	A/B	A/B	A/B	A/B	A/B	A/B	A/B	A/B	A/B	A/B	A/B	A/B	A/B	A/B	A/B	-	-	-
35D24S-F/R	PCR	A	B	A/B	A/B	A	A/B	A/B	A/B	A/B	A/B	A	A/B	A/B	A/B	A	-	-	-	-	-	-	-	-	A	-	-
57-F/R	PCR	A	B	A/B	A/B	A	A	A	A/B	A	A/B	A	A/B	A	A	A	A	A/B	A/B	A	A	A	A/B	A	A	-	-
Sc14398-F/R	RFLP	A	B	A/B	A/B	A	A	A	A/B	A	-	A	-	A	A	A	A	-	-	A	A	A	-	A	A	A	A
34C07T-F/R	PCR	A	B	A/B	A	A	A	A	A	A	A/B	A	A	A	A	A	A	A/B	A	A	A	A	A	A	A	A	A
67M09T-F/R	PCR	A	B	A/B	A	A	A	A	A	A	A	A	A	A	A	A	-	A	-	-	-	A	A	A	A	A	A
Sc337-3F/3R	RFLP	A	B	A/B	A	A	A	A	A	A	A	-	A	-	-	-	-	-	-	-	-	-	-	-	A	A	A
15A12T-F/R	RFLP	A	B	A/B	A	A	A	A	A	A	A	-	A	-	-	-	-	-	-	-	-	-	-	-	A	A	A
22C09T-F/R	RFLP	A	B	A/B	A	A	A	A	A	A	A	-	A	-	-	-	-	-	-	-	-	-	-	-	A	A	A
06E02S-F/R	RFLP	A	B	A/B	A	A	A	A	A	A	-	-	-	-	-	-	-	-	-	-	-	-	-	-	A	A	A
01K10S-F/R	RFLP	A	B	A/B	A	A	A	A	A	A	-	-	-	-	-	-	-	-	-	-	-	-	-	-	A	A/B	A
10M15S-F/R	RFLP	A	B	A/B	A	A	A	A	A	A	-	-	-	-	-	-	-	-	-	-	-	-	-	-	A/B	A/B	A/B
23J20T-F/R	RFLP	A	B	A/B	A	A	A	A	A	A	-	-	-	-	-	-	-	-	-	-	-	-	-	-	A/B	A/B	-
12E17T-F/R	RFLP	A	B	A/B	A	A	A	A	A	A	-	-	-	-	-	-	-	-	-	-	-	-	-	-	A/B	A/B	-
70B11T-F/R	RFLP	A	B	A/B	A	A	A	A	A	A	-	-	-	-	-	-	-	-	-	-	-	-	-	-	A/B	A/B	A/B
14C12T-F/R	RFLP	A	B	A/B	A	-	-	-	A	-	-	-	-	-	-	-	-	-	-	-	-	-	-	-	A/B	A/B	-
58F21S-F/R	RFLP	A	B	A/B	A	-	-	-	A	-	-	-	-	-	-	-	-	-	-	-	-	-	-	-	A/B	A/B	A/B
83J16S-F/R	RFLP	A	B	A/B	-	-	-	-	-	-	-	-	-	-	-	-	-	-	-	-	-	-	-	-	A/B	A/B	-

'A' indicates J150 homozygous, 'B' indicates No. 908 homozygous and 'A/B' indicates heterozygous genotype.

* Twenty three segregants are from about 500 BC_1 segregants in the cross of J150x(J150xNo.908).

1.3.2 Sequence analysis and expression of *nsd-2* candidate gene

One candidate gene was found in the annotation analysis used to search for expressed genes, proteins, and cDNAs in the deleted region. The full-length cDNA and corresponding genomic DNA sequences of this candidate were determined for strains No. 908 and J150 and compared each other (GenBank accession numbers of the full-length cDNA of No. 908 and J150 are AB365597 and AB365598, respectively). The deletion in J150 corresponded to the region from exons 5-13 in No. 908 (Fig. 1.3). This structure agreed with the difference in PCR product size shown in the genomic DNA (Fig. 1.2D) and messenger RNA (Fig. 1.4A), strongly suggesting that this gene is a candidate for *nsd-2*. The larger PCR products of lanes 6-9 in Fig. 1.2D came from the insertion of more than 3 kb in the intron between exons 7 and 8. The amplicon of lane 10 was much smaller than those generated from the other susceptibles (Figs. 1.2D and 1.4A). This could be explained by the presence of a deletion in the intron between exons 13 and 14 within to the primer sites located just after exon 13 and extending to the beginning of exon 14.

In RT-PCR using total RNA isolated from eight different tissues, the transcript was detected only in the midgut (Fig. 1.4B). The tissue specificity of this gene transcription was consistent with the unique characteristic that BmDNV-2 is able to infect only midgut (Kawase and Kurstak, 1991). For the developmental stage specificity, the RNA of the candidate gene was detected in the later stages of embryo and throughout the larval stages except during a molt (Fig. 1.4C). These results support the idea that this gene is expressed only after organogenesis of the midgut is completed and when the midgut is functional for digestion and absorption.

By NCBI-tBLASTx search, the cDNA sequence of the $+^{nsd-2}$ candidate from strain

No. 908 showed high homology with two amino acid transporter genes of *Manduca sexta* (GenBank accession nos. AF006063 with 77% and AF013963 with 76% identities) (Catagne et al., 1998; Feldman et al., 2000). Also the topology prediction method, SOSUI (http://bp.nuap.nagoya-u.ac.jp/sosui), predicted a membrane protein which encompasses 12 putative transmembrane domains (Fig. 1.5). In contrast, the translated protein of J150 could contain only the first three-pass transmembrane domains, because a significant portion of its coding region was deleted (Fig. 1.3). From these results, it was suggested that the deleted membrane protein structure is crucial for the infection of BmDNV-2. The homologous amino acid transporters of *M. sexta* transport specific amino acids (Catagne et al., 1998; Feldman et al., 2000). Whether the *nsd-2* candidate functions as an amino acid transporter is still unknown. However, it is clear that the *nsd-2* candidate is not essential for the silkworm, because the resistant strains that lack large portions of the internal sequence are healthy, with no detectable effect on development or other processes.

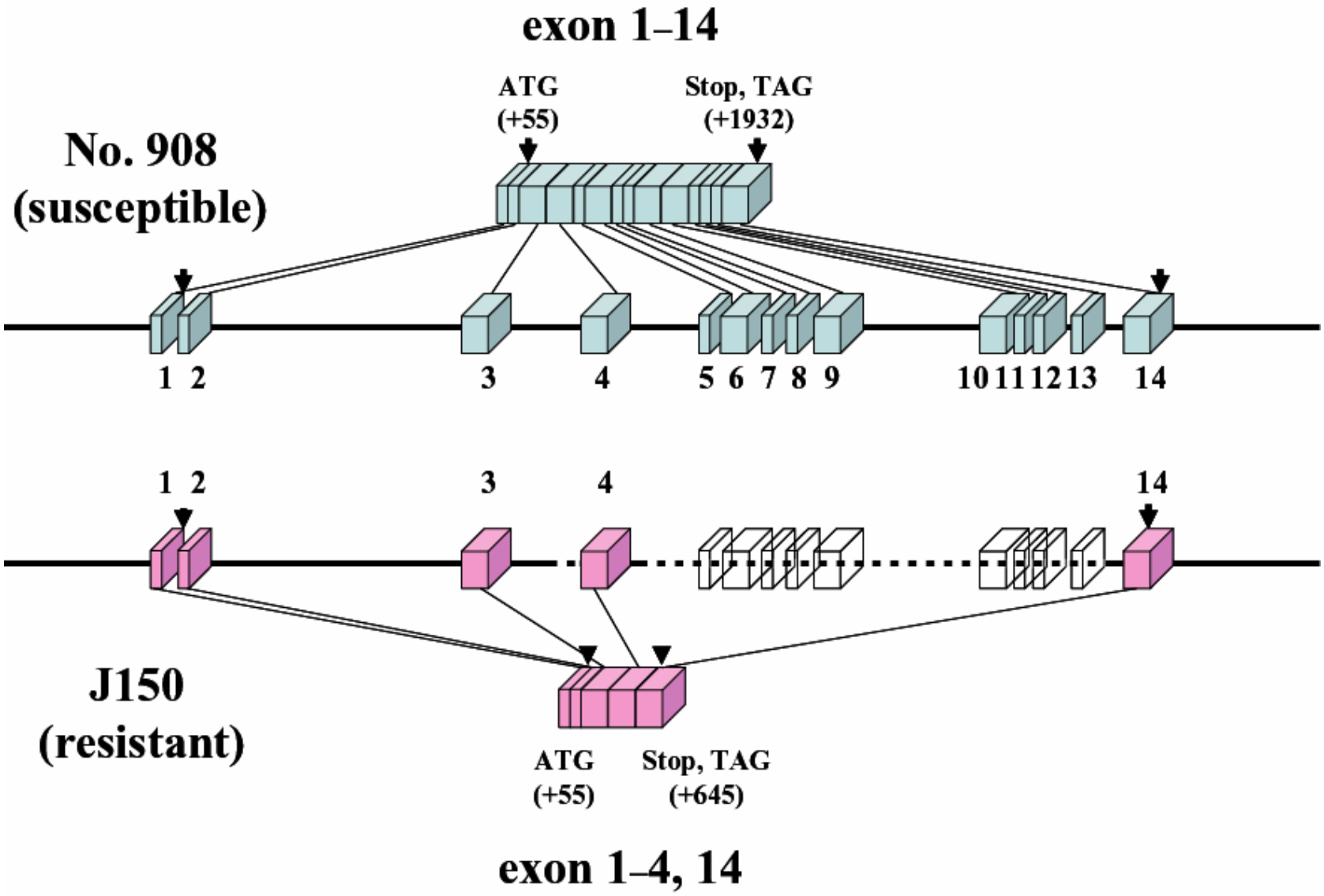
exon 1–14
ATG
(+55)
Stop, TAG
(+1932)
No. 908
(susceptible)
1 2
3
4
5 6 7 8 9
10 11 12 13
14
1 2
3
4
14
J150
(resistant)
ATG
(+55)
Stop, TAG
(+645)
exon 1–4, 14

Figure 1.3 Schematic genome structure of *nsd-2 and* $+^{nsd-2}$ candidate

Relative position and size of exon/intron in the genome of susceptible No. 908 (upper) and resistant J150 (lower). The dotted line indicates the deletion in the genome of J150. The arrows show the start and stop codons.

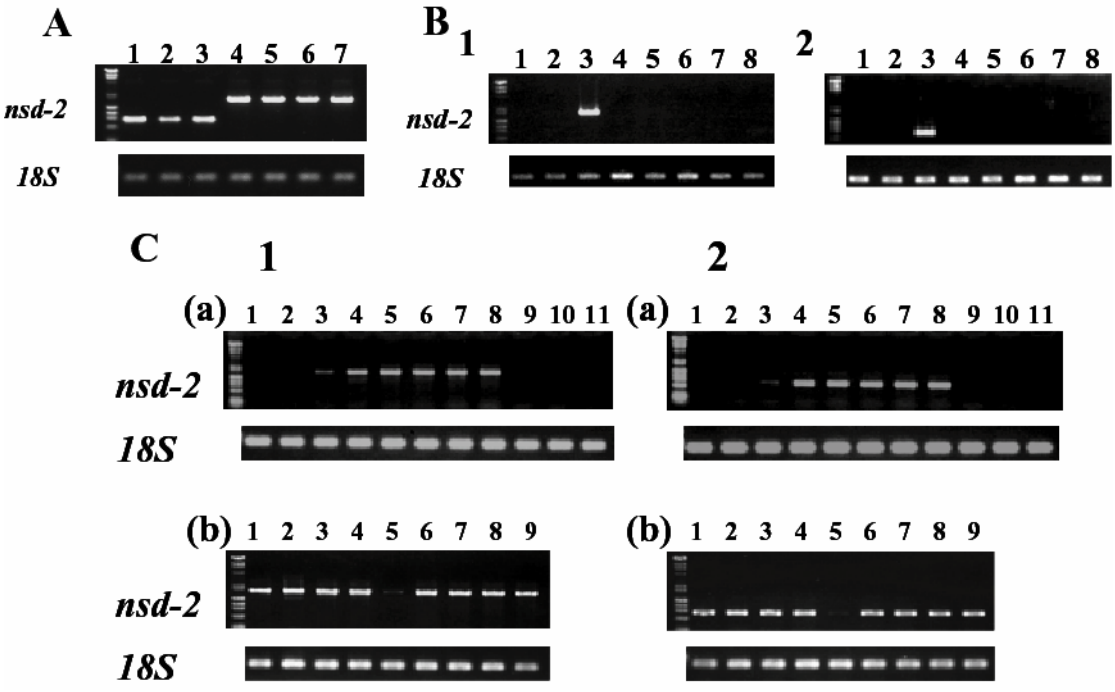

Figure 1.4 Expression of *nsd-2* detected by RT-PCR

(A) Expression of *nsd-2* candidate transcripts in the midgut of resistant and susceptible strains. Lane 1, J150; 2, J124; 3, No. 902; 4, No. 908; 5, C124; 6, p50T; 7, *B. mandarina*. Primer sets are for *nsd-2* and ribosomal *18S*, a positive control. 1–3, resistant; 4–7, susceptible. (B) Tissue specific expression of *nsd-2* in No. 908 (1) and J150 (2). Lane 1, silk gland; 2, foregut; 3, midgut; 4, hindgut; 5, Malpighian tubule; 6, fat body; 7, testis plus ovary; 8, central nervous system. (C) Stage-specific expression of *nsd-2* in No. 908 (1) and J150 (2). (a): Lanes 1–3, embryo, day 0, 4 and 10; 4–6, whole body, day 0 from first to third-instar larva; 7–8, midgut, day 0 from fourth and fifth-instar larva; 9–10, pupal gut, day 0 and 7; 11, adult gut, day 0. (b): Lanes 1–5, midgut, day 0, 1, 2, 3 and 4 of fourth-instar larva; 6–9, midgut, day 0, 2, 4, and 6 of fifth-instar larva.

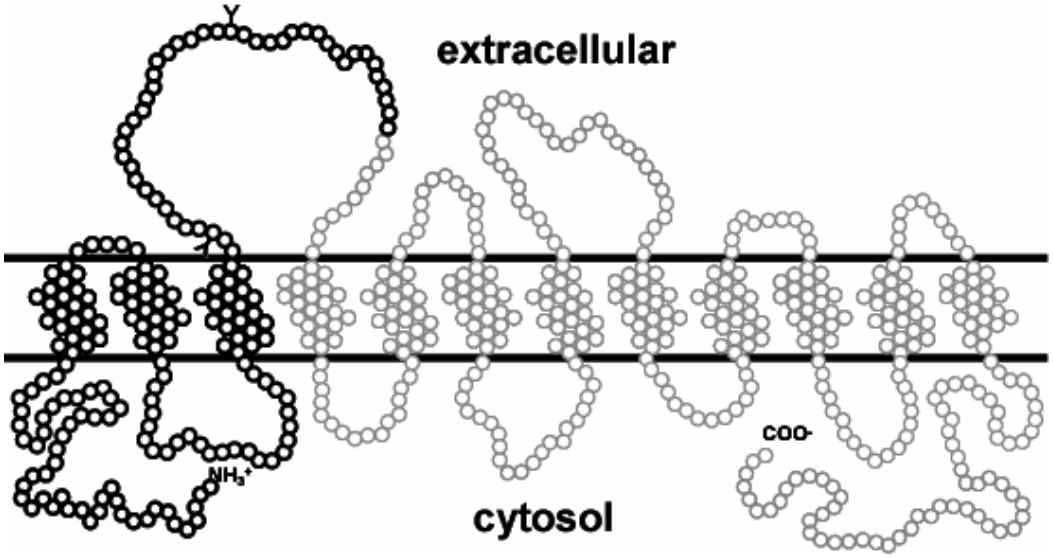

Figure 1.5 Hypothetical secondary structure of NSD-2

Two putative N-glycosylation sites ("Y" marks) are indicated between transmembrane domains 3 and 4. The gray region indicates the deletion in NSD-2. The secondary structure is based on the topology prediction method, SOSUI (http://bp.nuap.nagoya-u.ac.jp/sosui); the style of the diagram is based on a 12-pass membrane protein reported in *M. sexta* (Feldman et al., 2000).

1.3.3 Restoration of Virus-susceptibility by Germline Transformation of $+^{nsd-2}$ Gene to the Resistant Strain

To demonstrate that the candidate gene was responsible for virus resistance in the *nsd-2* mutant, I transformed resistant silkworms with the $+^{nsd-2}$ candidate sequence using the GAL4-UAS system to drive expression of the transgene and tested their susceptibility after inoculation with BmDNV-2 at first or fourth instar. After virus inoculation of the transgenic progeny of the four types of transgenic strains used for making the final construct (described in Materials and Methods), only the silkworms of the GAL4/UAS line (Fig. 1.1) showed a notable susceptibility phenotype, whereas the other lines grew up without any symptoms (Fig. 1.6A and Table 1.3). The GAL4/UAS line silkworms without BmDNV-2 inoculation did not change their growth (Fig. 1.6B). Using PCR to confirm that the transgene was inserted into the genome in the transgenic silkworms, the transgene-specific PCR product was detected in the GAL4/UAS and GAL4 lines (Fig. 1.7A). To confirm whether BmDNV-2 could multiply in the midgut of transgenic animals, BmDNV-2 DNA was detected by PCR using virus-specific primers (Abe et al., 1993). Only the GAL4/UAS lines had viral DNA (Fig. 1.7B). Moreover, by RT-PCR, the $+^{nsd-2}$ transcript was detected only in the GAL4/UAS line (Fig. 1.7C). These results indicated that the candidate gene is *nsd-2* itself, the virus resistance gene, and the wild type membrane protein expressed by the allele, $+^{nsd-2}$, is required for infection by BmDNV-2.

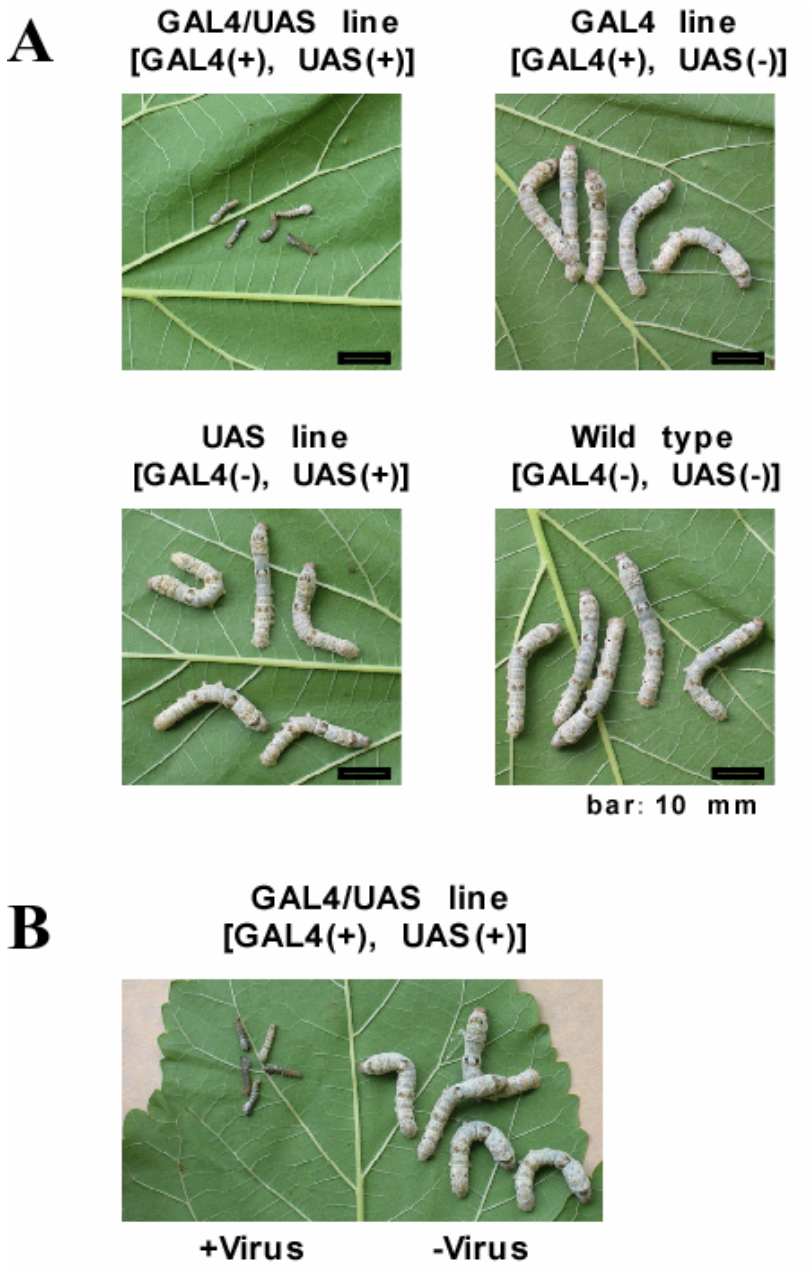

Figure 1.6 Viral inoculation tests using transgenic silkworms

(A) Transgenic silkworms of the GAL4/UAS line, GAL4 line, UAS line and wild type after the viral inoculation test. (B) Comparison of the GAL4/UAS line after exposure to BmDNV-2 at day 0 of first instar (left) and unexposed control (right). The larvae started to die from 7 days after inoculation (at second to third instar). The pictures were taken at the fourth instar.

Table 1.3. Virus inoculation of the transgenic silkworms.

Experiment	Line	Genotype	No. of silkworms used for the virus inoculation	No. of surviving silkworms	No. of dead silkworms
1	GAL4/UAS	GAL4(+), UAS(+)	25	0	25
	GAL4	GAL4(+), UAS(-)	24	24	0
	UAS	GAL4(-), UAS(+)	14	14	0
	wild type	GAL4(-), UAS(-)	5	5	0
2	GAL4/UAS	GAL4(+), UAS(+)	31	0	31
	GAL4	GAL4(+), UAS(-)	40	40	0
	UAS	GAL4(-), UAS(+)	41	41	0
	wild type	GAL4(-), UAS(-)	38	38	0

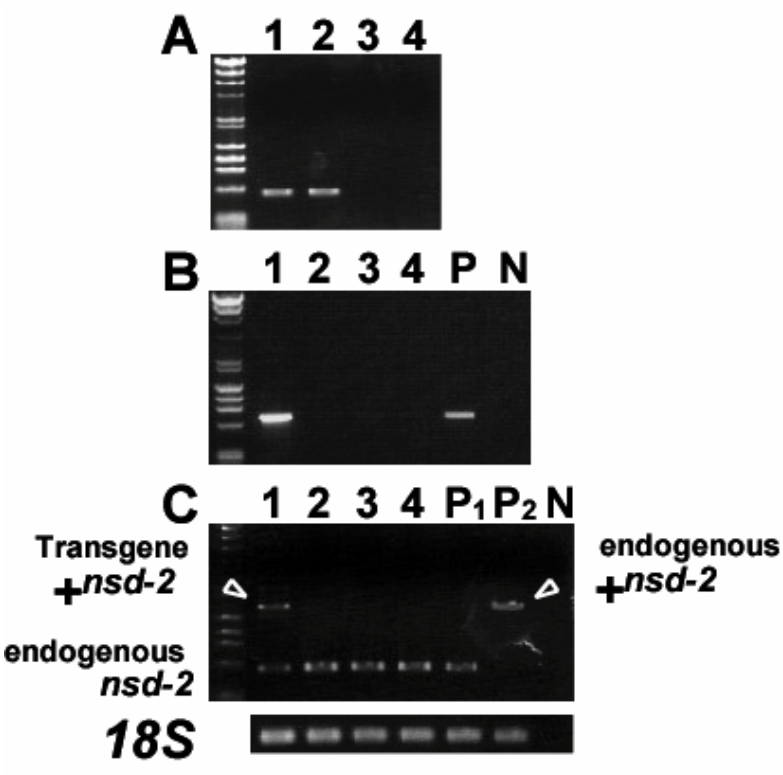

Figure 1.7 PCR and RT-PCR analysis of the transgene

(A) PCR analysis of the introduced gene from 4 transgenic lines. (B) Detection of BmDNV-2 from the midgut of 4 transgenic lines with primers based on the virus genome sequence. (C) Expression pattern of the introduced gene, $+^{nsd-2}$, from the midgut of 4 transgenic lines. Lanes 1-4, GAL4/UAS, GAL4, UAS lines and wild type, respectively; P, virus inoculation solution as a positive control; P1 and P2, midgut of J150 and No. 908 as positional markers; N, negative control template. The white arrowheads indicate the PCR products of $+^{nsd-2}$.

1.4 Discussion

In this study, by means of positional cloning using *B. mori* genome information (Kadono-Okuda et al., 2002; Mita et al., 2004; Xia et al., 2004; Nguu et al., 2005; Yamamoto et al., 2006), I carried out the isolation of *nsd-2*, a putative transporter gene, and showed that a deletion of the region corresponding to 9 out of 12 predicted transmembrane domains confers resistance to BmDNV-2. This is the first report of the isolation of a mutant gene in the silkworm by this strategy. Moreover, to the best of my knowledge, this is the first report of the isolation of a mutant gene that causes absolute resistance to a virus in insects.

Infection mechanisms have been reported in human parvovirus, B19 (Brown et al., 1993), canine parvovirus and feline panleukopenia virus (Palermo et al., 2003). The relationship between each virus and its receptor is very specific; specific amino acids both on the viral surface and on the exposed domain of the receptor are important for binding (Palermo et al., 2003). From these reports, I think that the complete membrane protein functions as a receptor for BmDNV-2, and the site that the virus recognizes as a target is present in the deleted portion of the membrane protein, *nsd-2*. It is still not clear how BmDNV-2 interacts with the membrane protein. It would be of great importance to determine the recognition sites of BmDNV-2 and *nsd-2*. Many viruses of Densovirinae are known to infect diverse insect groups such as *B. mori*, *J. coenia*, and *G. mellonella* in Lepidoptera; *A. aegypti* in Diptera; and *P. fuliginosa* in Blattodea, as well as in crustaceans such as lobster and crab (Bergoin and Tejissen, 2000). There are many reports on the relationship between densoviruses and their host range or tissue specificities (Kawase and Kurstak, 1991). However, the factors controlling host and tissue specificity are still unknown. *nsd-2* is the first report of the critical host factor for the infection of insect viruses, including Densoviruses. Although BmDNV-2 has been

excluded from Densovirinae, it has distinctive pathological characters in common with BmDNV-1, such as an infective tissue of midgut columnar cell nuclei and the existence of well defined resistant and susceptible *Bombyx* strains. The discovery of *nsd-2* will contribute to the analysis of the infection mechanism in other densoviruses. What are the targets for the other densoviruses that can infect many tissues, like JcDNV or have a broad host range like JcDNV and AeDNV? The answers to these questions must be of great interest.

B. mandarina, which is considered to have a common ancestor to *B. mori* (Goldsmith et al., 2005), is susceptible (Figs. 1.2D and 1.5A). Chinese, Indian and Japanese native (ancient) strains also tend to be susceptible; however, many genetically improved Japanese strains are resistant (Furuta, 1994; Furuta, 1995). Therefore, this form of DNV-2 resistance may be an acquired mutation through silkworm breeding improvement. In contrast, considering that the susceptibility to DNV-1 is reversed (Furuta, 1994), DNV-2 is likely to be a native disease of *Bombyx*, whereas the origin of DNV-1 is likely to be from pathogens of other insects. With the availability of the complete genome sequence of *B. mori* (Mita et al., 2004; Xia et al., 2004), identification of other BmDNV resistance genes, *Nid-1*, *nsd-1* and *nsd-Z* is expected in the near future. A study of the relationship between the gene described here and the other BmDNV resistance genes is of interest, in part because it can reveal new findings on the infection mechanism of BmDNV. The results of our study will contribute to research not only on insect pathogenic viruses important to sericulture and for agricultural pest control but also for other viruses transmitted by insects (Carlson et al., 2006). Although most virus receptors are essential for their hosts, it is of interest that, apparently, this one is not. In addition to the present gene, I found another similar gene that has no relationship with

viral resistance (unpublished data). Although it is not known whether the second gene takes over a role in amino acid transport, having an extra copy might accelerate the mutation of the other and lead to its becoming resistant. The recently reported rapid emergence of field resistance to baculovirus in codling moth (Asser-Kaiser et al., 2007) is consistent with this kind of scenario.

Chapter 2

Positional cloning and functional analysis of the resistance gene, *nsd-1*, to the *Bombyx mori* densovirus type-1 (BmDNV-1)

2.1 Introduction

Bombyx mori densovirus (BmDNV) is classified into *B. mori* densovirus type-1 (BmDNV-1) and type-2 (BmDNV-2) according to the difference of the infectivity, the serological characteristics for the silkworm, and the genome structure (Watanabe and Maeda, 1978; Seki, 1984; Watanabe et al., 1986). BmDNV-1 and BmDNV-2 belonged to a member of the genera Iteravirus and Bidensovirus within the family Parvoviridae. Recently, it is proposed that BmDNV-2 should be excluded from the family Parvoviridae, because of the divided genomes and a DNA polymerase motif in its own genome (Tattersall et al., 2005).

It has been shown that certain silkworm strains are highly susceptible, while other strains are nonsusceptible to BmDNVs even though they are fed a high concentration of virus inocula (Watanabe and Maeda, 1978; Watanabe and Maeda, 1981; Seki, 1984). Nonsusceptibility to DNV-1 is controlled by two genes, *Nid-1* (Non-infectious to densonucleois virus) and *nsd-1* (non-susceptibility to densonucleosis virus type-1) (Watanabe and Maeda, 1981; Eguchi et al., 2007). *Nid-1* has been mapped to the position 31.1 cM on linkage group 17 (Eguchi et al., 2007), and *nsd-1* has been mapped on linkage group 21 at 8.3 cM (Eguchi et al., 1991). Genetic experiments also revealed that *Nid-1* is epistatic to $+^{nsd-1}$ (Abe et al., 1987). Although these two mutations have been mapped with phenotypic and DNA markers, their responsible genes have not been identified.

In Chapter 1, I have conducted the identification of the mutant gene, *nsd-2* by positional cloning and found that *nsd-2* encodes a putative amino acid transporter, which may function as a receptor for BmDNV-2. In this chapter, I attempted to isolate the *nsd-1* mutant gene with the same approach. By positional cloning, I identified a novel mucin-like gene as the *nsd-1* candidate and performed functional analysis of this

gene using biochemical and immunohistochemical techniques.

2.2 Materials and Methods

2.2.1 Silkworm strains, cell lines, and virus infection

I used silkworm strains resistant to BmDNV-1, B (Hokkaido University), p50T, C108T (The University of Tokyo), C124, No. 104, No. 115, No. 138, No. 141, No. 603, No. 902, and No. 910 (National Institute of Agrobiological Sciences, NIAS), and susceptible strains, J02, J124, J150, No. 101, No. 102, No. 122, No. 123, No. 126, No. 133, No. 142, No. 144, No. 146, and No. 918 (NIAS). For linkage analysis, single-pair backcrosses (BC_1) between p50T females and F_1 males (J124 female × p50T male), and between p50T females and F_1 males (p50T female × J150 male) were used. All silkworm strains were reared at 25°C.

The BmN-4 (BmN) cells were cultured at 27°C in IPL-41 medium (Gibco) supplemented with 10% fetal bovine serum as described previously (Katsuma et al., 2007).

The newly-ecdysed fourth instar larvae were fed mulberry leaves smeared with BmDNV-1 suspension as described previously (Abe et al., 1998).

2.2.2 Positional cloning

Positional cloning of the *nsd-1* mutant gene was performed as described in Chapter 1. For positional cloning, polymerase chain reaction (PCR) and single nucleotide polymorphism (SNP) markers were generated at each position on linkage group 21, and the markers which showed polymorphism between the parents were used for linkage analysis of 1,941 BC_1 larvae selected with virus inoculation from about 4,000 individuals. The primer sequences used are shown in Table 2.1.

Table 2.1. The primers used in this research.

object	name	sequence (5' - 3' end)
linkage analysis in Table 2.2	T059O10-F	GATAGTGGTGCGCGTGGT
	T059O10-R	GACGACGAGCCGTGGTAG
	T024K22-F	GCAAAAGCCATTATTCTATTTTCA
	T024K22-R	TGAACAAAAGTAATTTAATAATAGCCC
	T018B21-F	GTCTACGGAAGCGTCAAAGC
	T018B21-R	GCGAAGCACGAATCTTCTTT
	Sc14272-89J19T-F	TTTATTTCAGCGGATTCGGTATTTG
	Sc14272-89J19T-R	TTTAATTGGATCCACGGTATTGGAA
	Sc3970-52D14T-F	GACACTAATGGGTTCGTTCATGTCC
	Sc3970-52D14T-R	TTTTGCACCTTTCTTTTGTTTGTTGA
	Sc8241-62B09T-CF	TAAGAACATTAAGAAAGCCTTAATGC
	Sc8241-62B09T-CR	GCCCTTTATTTATGTTTAGGTTACC
	T062B09-F	TTCGCTTATGTGTCCGTGAA
	T062B09-R	GGACCACGCCTATCACACC
	Sc6678-09B04T-F	GGGTGAGGTCCGTTTAAATCAAATACT
	Sc6678-09B04T-R	CCTGCCCATTACTTTTGAGACTTCA
	BGIBMGA001597-F	TGCAAGTATTACACGGAAAGAACTC
	BGIBMGA001597-R	AAGTGACCAATCGTGTAGTATTACG
	Sc10109-48J16S-F	GACACTGGATGTTAAGGGATCACCA
	Sc10109-48J16S-R	CTCGCTATCTAGGTGCACGAACAAT
	T605G10-F	TGTTTTGGACATATCCTGCG
	T605G10-R	CATCCGTGAAAACCACTGTAGA
	T611D06-F	TTTGTTTTGGACGCGAGATT
	T611D06-R	TTCGTTCAGGGAATTGATGA
RT-PCR of *nsd-1* candidate	BGIBMGA001388-F	TCTTCGACAATGAAACTGCAAATCA
	BGIBMGA001388-R	TTGTTTACGCGTTCGCTCTTCATAC
	BGIBMGA001389-F	TGATGAAGTTGCAAATCGTTGTGTT
	BGIBMGA001389-R	TTCATGCGGAGATTGACGAAGTTAT
	BGIBMGA001390-F	CAGTAGAACCTTCGTTTGACCATCG
	BGIBMGA001390-R	GGACAGTGATGTAGCCATGAAACCT
	BGIBMGA001596-F	ATTACTCATGGAGGCGCTAACCAAT
	BGIBMGA001596-R	GTCACTTCCAGAGATGAACGAGGTC
	BGIBMGA001597-F	TGCAAGTATTACACGGAAAGAACTC
	BGIBMGA001597-R	AAGTGACCAATCGTGTAGTATTACG
	18S-sense	TTGACGGAAGGGCACCACCAG
	18S-antisense	GCACCACCACCCACGGAATCG
Construction of plasmids containing mutant *nsd-1*	*nsd-1* -F	TTGGGACGTGCTGGAATATTTATTAGAA
	nsd-1 -R	GATATTGCTTGGTTGTGGCTCGATACT
	nsd-1 -mutation-1F	CAACTACAGTCaAGACTGAGCCTC
	nsd-1 -mutation-1R	GAGGCTCAGTCTtGACTGTAGTTG
	nsd-1 -mutation-2F	CGTCTCAGAGgGCAACAACCCAG
	nsd-1 -mutation-2R	CTGGGTTGTTGCcCTCTGAGACG
Construction of bacterial expression vectors	pET-F	GGATCCGGGGCAGAGGAATCGGCTCACG
	pET-R	CTCGAGAGCTGCATAGCCCATTAACTGGAG
Construction of BmN cells stably expressing His-tagged NSD-1	NSD-1-pIZ-F	GGATCCATGAATTCAACCGCGTGCAAGTATTAC
	NSD-1-pIZ-R	TCTAGATTAATGATGATGATGATGAGCTGCATAGCCCATTAACTGGA

2.2.3 Isolation of genomic DNA and total RNA

Genomic DNA was isolated from a small portion of the body (eg. caudal end of the abdomen) from fifth instar larvae using DNAzol (Invitrogen) according to the manufacturer's protocol. Day 1 fifth instar larvae were used for the isolation of total RNA from individual tissues, including silk gland, foregut, midgut, hindgut, Malpighian tubule, fat body, testis plus ovary, and central nervous system. In the isolation of total RNA from individuals of different stages, eggs of day 0, 4, and 8, whole body from day 0 of first instar to fourth instar larvae, midgut from day 1, 2, and 3 of fourth instar, midgut from day 0, 2, 4 and 6 of fifth instar, midgut from day 0, 5 of pupae and day 0 of adults were used. Total RNA was purified using Trizol (Invitrogen), reverse-transcribed using Oligo $(dT)_{12\text{-}18}$ primer (Invtrogen) and Superscript III reverse transcriptase (Invitrogen) according to the manufacturer's protocol. Full length cDNAs were cloned using a SMART RACE cDNA Amplification Kit (Clontech) according to the manufacturer's protocol.

2.2.4 PCR and reverse transcription PCR (RT-PCR) analysis

PCR was performed using Ex Taq (TaKaRa) and primer sets designed based on the SNP linkage map (Yamamoto et al., 2006; Yamamoto et al., 2008) and the *B. mori* genome sequence information (Mita et al., 2004; Xia et al., 2004) (Table 2.1). The PCR conditions were as follows: initial denaturation at 94°C for 2 min, 35 cycles at 94°C for 15 s, 60°C for 15 s, and 72°C for 1 min, followed by 72°C for 4 min. RT-PCR was performed using Ex Taq (TaKaRa) and primer sets designed with the ORF of the candidate gene (Table 2.1). The PCR conditions were as following: initial denaturation at 94°C for 2 min, 30 cycles at 94°C for 15 s, 60°C for 15 s, and 72°C for 1 min,

followed by 72°C for 4 min.

2.2.5 Functional annotation

The candidate genes in the region narrowed by linkage analysis were functionally annotated using KAIKObase (http://sgp.dna.affrc.go.jp/KAIKObase), KAIKO blast (http://kaikoblast.dna.affrc.go.jp), KAIKOGAAS (http://kaikogaas.dna.affrc.go.jp), and NCBI blast (http://blast.ncbi.nlm.nih.gov/Blast.cgi).

2.2.6 Sequencing of the *nsd-1* candidate genes

To examine the sequences of the *nsd-1* candidate genes, we performed RT-PCR using the cDNA prepared from midgut from day 1 of fourth instar larvae of resistant (p50T) and susceptible (J124) strains. The primer sets for PCR of the five *nsd-1* candidate genes (China gene model BGIBMGA001388, BGIBMGA001389, BGIBMGA001390, BGIBMG001596, and BGIBMG001597) are shown in Table 2.1. RT-PCR was performed using ExTaq (TaKaRa) under the following conditions: initial denaturation at 94°C for 2 min, 30 cycles at 94°C for 15 s, 60°C for 15 s, and 72°C for 1 min, followed by 72°C for 4 min. The PCR products were subcloned into pSTBlue-1 AccepTor vector (Novagen) and sequenced by ABI 3730xl DNA analyzer (Applied Biosystems). Ribosomal 18S RNA was used as a control in all PCR experiments (Gopalapillai et al., 2006).

2.2.7 Construction of plasmids containing mutant *nsd-1*

To clone the *nsd-1* candidate gene, we performed RT-PCR using the cDNA prepared from midgut from day 1 fourth instar larvae of resistant (p50T) and susceptible (J124)

strains, and primer set *nsd-1*-F and *nsd-1*-R (Table 2.1). RT-PCR was performed using ExTaq (TaKaRa) under the following conditions: initial denaturation at 94°C for 2 min, 30 cycles at 94°C for 15 s, 60°C for 15 s, and 72°C for 1 min, followed by 72°C for 4 min. The PCR products were subcloned into pSTBlue-1 AccepTor vector (Novagen) and sequenced by ABI 3730xl DNA analyzer (Applied Biosystems). Four types of cDNAs, NSD-1-Res-nonsp (a non-spliced form of the resistant strain p50T), NSD-1-Sus-nonsp (a non-spliced form of the susceptible strain J124), NSD-1-Res-sp (a spliced form of the resistant strain p50T), and NSD-1-Sus-sp (a spliced form of the susceptible strain J124) were cloned.

To construct plasmids containing point mutations, two-step PCR-based mutagenesis was performed using four cDNA constructs described above as a template (Daimon et al., 2005). Primers used in the mutagenesis experiments are shown in Table 2.1. Four mutant PCR products, NSD-1-K110E-nonsp (K110), NSD-1-G118R-nonsp (G118R), NSD-1-K85E-sp (K85E), and NSD-1-G93R-sp (G93R) were subcloned into the pSTBlue-1 AccepTor vector and sequenced by ABI 3730xl DNA analyzer.

2.2.8 Prediction of the motif of NSD-1

The motif in amino acid sequence of NSD-1 was searched using NCBI-blastp (http://blast.ncbi.nlm.nih.gov/Blast.cgi), MOTIF (http://motif.genome.jp), and SOSUI (http://bp.nuap.nagoya-u.ac.jp/sosui).

2.2.9 Generation of the NSD-1 antibody

Expression and purification of a recombinant NSD-1 protein were performed as described previously (Meng et al., 2009). To construct a bacterial expression vector, the

coding region corresponding to amino acids 42-155 of NSD-1 was amplified by PCR with a primer set pET-F and pET-R (Table 2.1) using NSD-1Res-nonsp as a template. PCR products were digested with *Bam*HI and *Xho*I, inserted into the pET24b vector (Novagen), and introduced into *Escherichia coli* strain BL21(DE3) competent cells. NSD-1 expression was induced by the addition of isopropyl-1-thio-β-D-galactopyranoside (IPTG) to a final concentration of 1 mM. The transformants were cultured at 37°C for 3 hr after IPTG induction. The cells were collected by centrifugation and suspended in 10 ml of B-PER bacterial protein extraction reagent (Pierce) containing a cocktail of proteinase inhibitors (Roche). The supernatant was collected by centrifugation (8,000 rpm, 4°C, 15 min). The inclusion body was solubilized with 25 ml of urea buffer (50 mM Tris-HCl, 500 mM NaCl, 8 M urea, pH 8.0), and the supernatant was collected by centrifugation (8,000 rpm, 4°C, 15 min). His-tagged NSD-1 was purified using the His GraviTrap nickel affinity column (GE Healthcare) according to the manufacturer's protocol. After the column was equilibrated with 10 ml of binding buffer (20 mM sodium phosphate, 500 mM NaCl, 20 mM imidazole, pH 7.4), a protein sample was loaded onto the column and washed with 10 ml of the binding buffer. Elution was performed using an elution buffer (20 mM sodium phosphate, 500 mM NaCl, 100 mM imidazole, pH 7.4). The eluate was concentrated from 30 to 7 ml using Centriprep YM-30 (Amicon). The protein concentration was determined using the method of Bradford (Bradford, 1976). An antiserum against recombinant NSD-1 was raised in rabbits.

2.2.10 Generation of BmN cells stably expressing His-tagged NSD-1

The coding regions of NSD-1 with a His-tag sequence at the C-terminus were amplified

by PCR with the primer set NSD-1-pIZ-F and NSD-1-pIZ-R using various cDNA constructs as templates. PCR products were digested with *Bam*HI and *Xba*I, and ligated into the pIZ/V5-His vector (Invitrogen). This vector possesses the *ie2* promoter of *Orgyia pseudotsugata* nucleopolyhedrovirus for the constitutive expression of the gene of interest and the zeocin-resistant gene for selection of stable cell lines. BmN cells were transfected with pIZ/V5-His or NSD-1-His-pIZ using Cellfectin reagent (Invitrogen). Two days after transfection, zeocin (final concentration, 500 μg/ml) was added into the medium. At 2 weeks after drug selection, we verified the expression of His-tagged NSD-1 by Western blot analysis.

2.2.11 Preparation of the cell membrane fraction

BmN cells stably expressing His-tagged NSD-1 were washed three times in phosphate-buffered saline (PBS) and harvested from 60-mm diameter plates by scraping. Cells were collected with 1 ml PBS in the presence of a cocktail of proteinase inhibitors (Roche), sonicated for 5 s at 4°C using a SONIFIRE Model 250 (BRANSON, Danbury, CT), and then incubated on ice for 30 s. The sonication steps were repeated five times. Large debris was cleared by centrifugation at 3,000 × g for 10 min at 4°C. The resulting microsomal supernatant was spun at 20,500 × g for 30 min at 4°C, and the pellet was collected as membrane protein fraction.

The midgut was prepared from day 3 fifth instar larvae of p50T, and 10 volume of PBS containing a cocktail of proteinase inhibitors (Roche) was added. The midgut was homogenized using the tight-fitting pestle. Large debris was cleared by centrifugation at 3,000 × g for 10 min at 4°C. The resulting microsomal supernatant was spun at 20,500 × g for 30 min at 4°C, and the pellet was used as membrane fraction.

2.2.12 Analysis of NSD-1 glycosylation

Asparagine-linked polysaccharides (N-linked glycans) and threonine/serine-linked polysaccharides (O-linked glycans) were removed from membrane samples using PNGase F (New England Biolabs) and O-Glycosidase from *Streptococcus pneumoniae* (SIGMA), respectively, according to the manufacturer's protocol. Glycosylation of NSD-1 after enzyme treatment was examined by Western blotting.

2.2.13 Sodium dodecyl sulfate-polyacrylamide gel electrophoresis (SDS-PAGE) and Western blot analysis

SDS-PAGE and Western blot analysis were performed as described previously (Daimon et al., 2005). The protein concentration was determined using the Coomassie Plus Protein Assay (Pierce) with bovine serum albumin as a standard. Western blot was performed as follows: after SDS-PAGE, the proteins were blotted onto polyvinylidene fluoride (PVDF) membrane (Immobilon-P, Millipore) using a blotting apparatus (ATTO) in a transfer buffer (25 mM Tris, 192 mM Glycine, 20% methanol). The membrane was incubated for TBS-T buffer (20 mM Tris-HCl pH 8.0, 150mM NaCl, and 0.05% Tween 20) containing 4% Blockace (Dainihon Pharmaceutics) followed by 1 hr incubation at room temperature with Penta-His antibody (QIAGEN, 1:5000 dilution in TBS-T) or anti-NSD-1 antibody (1:10,000 dilution in TBS-T). The blot was incubated with the goat anti-mouse or rabbit horseradish peroxidase-conjugate secondary antibody (Zymed laboratory, 1:5000 dilution in TBS-T) for 1 hr at room temperature. Signals were detected with the ECL kit (Amersham) and visualized using the LAS1000 Plus Imaging System (Fuji Film).

2.2.14 Immunohistochemistry

The immunohistochemical analysis was performed as described previously (Daimon et al., 2005). The larvae at the feeding stage (day 3 of fifth instar larvae) were fixed with a FAA solution (4% formaldehyde, 0.5% acetic acid, and 45% ethanol) overnight at 4 °C. Samples were dehydrated through ascending grade of ethanol, embedded in paraffin, and then cut into 10 μm thick serial sections. The slides hydrated through ethanol series were incubated with TBS-T for 5 min and then with a blocking buffer (TBS-T containing 5% skim milk) for 1 h at 25°C. After blocking, the slides were incubated with the primary antibody diluted in TBS-T containing 5% skim milk for 1 h at 25°C, then with the secondary antibody diluted in TBS-T containing 5% skim milk at 25°C. The primary antibody was anti-NSD-1 at a dilution of 1:200, and the second antibody was an AlexaFluor488-labeled goat anti-rabbit IgG $F(ab)_2$ fragment (Molecular Probes) at a dilution of 1:200. Subsequently, the sections were counter-stained with a 4', 6-diamidino- 2-phenylindole dihydrochloride solution (DAPI, Wako) at a dilution of 1:1,000 in TBS-T for 5 min. Fluorescence was observed under a fluorescence microscope (Olympus BX51) and photographed. For control experiments, pre-immune sera were also used at a dilution of 1:200, following the procedure described above.

2.3 Results

2.3.1 Linkage mapping of the *nsd-1* mutant gene

To identify a candidate region for the *nsd-1* mutant gene, I performed a genetic linkage analysis using the primer sets designed based on SNP linkage map (Yamamoto et al., 2006) and the *B. mori* genome sequence information (Mita et al., 2004; Xia et al., 2004) (Table 2.1). First, I roughly mapped the mutant gene using 187 BC_1 individuals, and narrowed the *nsd-1* linked region to between the T7 end of BAC clone 089J19 and the T7 end of BAC clone 605G10 (Fig. 2.1). This region was 1.8 cM in length according to the SNP map (Yamamoto et al., 2006). I further narrowed this region to between the position 7,402,527 nucleotide (nt) and 7,799,223 nt on Bm_scaf7 using about 2,000 BC_1 individuals. The region was about 400 kb in length (Fig. 2.1 and Table 2.2).

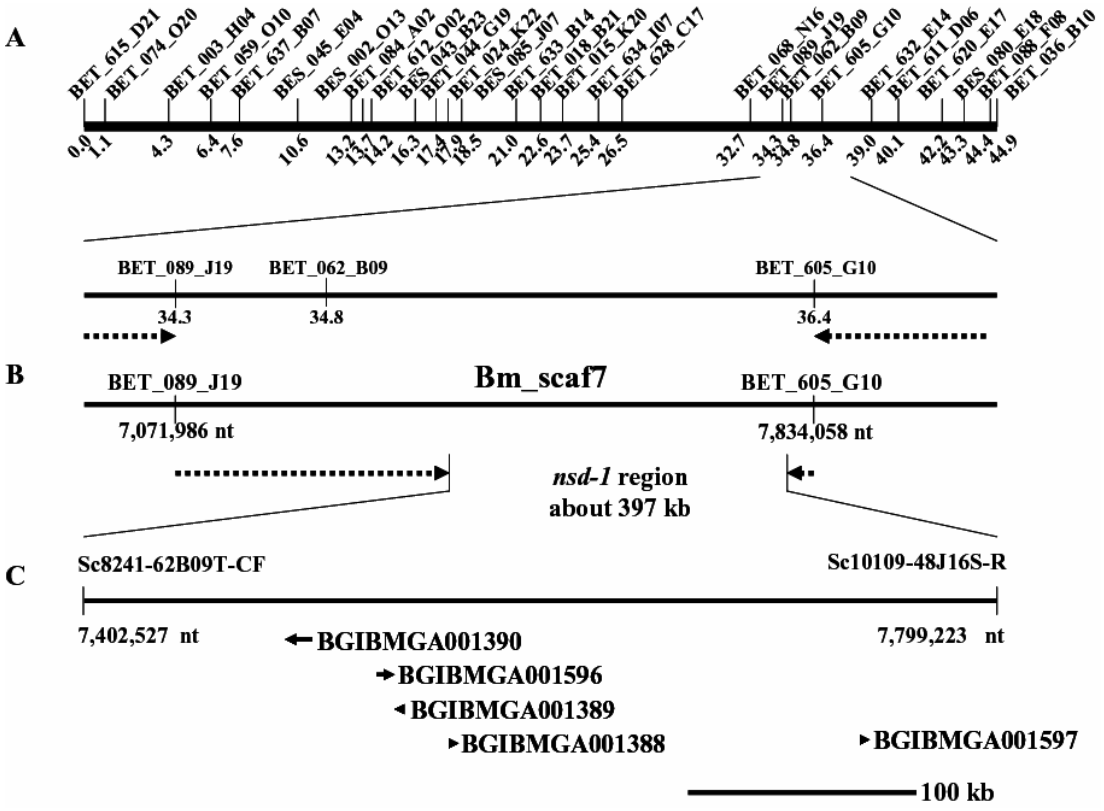

Figure 2.1 Mapping of the *nsd-1* mutant gene on linkage group 21

(A) SNP markers and linkage analysis. Upper figure indicates the positions of SNP markers from BAC end sequences. The distance is shown in centiMorgan units (cM). In the lower figure, a dotted line indicates the result of a rough mapping to narrow the region linked to the *nsd-1* mutant gene. (B) Bm_scaffold on the narrowed region and fine mapping. A dotted line indicates the result of the detailed linkage analysis to narrow the region linked to the *nsd-1* mutant gene. (C) Gene annotation in the *nsd-1* linked region. Five predicted genes, BGIBMGA001388, BGIBMGA001389, BGIBMGA001390, BGIBMG001596, and BGIBMG001597 are shown.

Table 2.2. Linkage analysis of BC_1 segregants.

primer sets	method	p50T	J124 or J150	F_1	BC_1*	
T059O10-F/R	sequence	A	B	A/B	A/B	A
T024K22-F/R	sequence	A	B	A/B	A/B	A
T018B21-F/R	sequence	A	B	A/B	A/B	A
Sc14272-89J19T-F/R	sequence	A	B	A/B	A/B	A
Sc3970-52D14T-F/R	sequence	A	B	A/B	A/B	A
Sc8241-62B09T-CF/C	sequence	A	B	A/B	A/B	A
T062B09-F/R	sequence	A	B	A/B	A	A
Sc6678-09B04T-F/R	PCR	A	B	A/B	A	A
BGIBMGA001597-F/F	sequence	A	B	A/B	A	A
Sc10109-48J16S-F/R	PCR	A	B	A/B	A	A/B
T605G10-F/R	sequence	A	B	A/B	A	A/B
T611D06-F/R	sequence	A	B	A/B	A	A/B

'A' indicates p50T homozygous, 'B' indicates J124 or J150 homozygous and 'A/B' indicates heterozygous genotype.

* Inlinkage analysis about 2000 BC_1 individuals with the nsd-1 phenotype were used.

2.3.2 Identification of the *nsd-1* candidate gene

I predicted five candidate genes (China gene model BGIBMGA001388, BGIBMGA001389, BGIBMGA001390, BGIBMG001596, and BGIBMG001597) by gene model search. First, I examined whether these five candidate genes are expressed in the midgut where BmDNV-1 can infect and replicate. RT-PCR analysis showed that expressions of two of the five genes (BGIBMGA001390 and BGIBMGA001597) were detected in the midgut. Next, we cloned and sequenced two candidate genes and compared the sequences between resistant (C124 and p50T) and susceptible (J124 and J150) strains. In the ORF of BGIBMGA001390, I did not find any differences between resistant and susceptible strains. On the other hand, two nucleotide substitutions, both of which resulted in amino acid substitution at residues 110 (K110E) and 118 (G118R), were observed in the ORF of BGIBMGA001597 (Figs. 2.2A, B). Based on these results, we speculated that this gene, BGIBMGA001597, corresponds to the *nsd-1* mutant gene.

A

```
1'  ATGAATTCAA CCGCGTGCAA GTATTACACG GAAAGAACTC TGGGTTGGAT GTTGAACAAC AAAACGATAG TGTTTCTTTC
    ********** ********** ********** ********** ********** ********** ********** **********
1"  ATGAATTCAA CCGCGTGCAA GTATTACACG GAAAGAACTC TGGGTTGGAT GTTGAACAAC AAAACGATAG TGTTTCTTTC

81'  ATTACTGTCA TTCTGTTTGT TTGTTTCGAC GTTAGCGTTG GCCGCGCAGA CGAATCGCCT CACGGCCGAG GTGGACGATC
     ********** ********** ********** ********** ********** ********** ********** **********
81"  ATTACTGTCA TTCTGTTTGT TTGTTTCGAC GTTAGCGTTG GCCGCGCAGA CGAATCGCCT CACGGCCGAG GTGGACGATC

161'  TCAGCCACCG TTTGACCACG TCTTCTGTTC TGGAAACTAC AACACCAATC AACGTAGACA CAACAACTAC TACAGAAGGT
      ********** ********** ********** ********** ********** ********** ********** **********
161"  TCAGCCACCG TTTGACCACG TCTTCTGTTC TGGAAACTAC AACACCAATC AACGTAGACA CAACAACTAC TACAGAAGGT

241'  CAGACTACTA CAGATTCAAC AATTACTACT ACGGATGCTC AAACTTCTAC TGATTCAACG ATTACTACTA CAGATTCAAC
      ********** ********** ********** ********** ********** ********** ********** **********
241"  CAGACTACTA CAGATTCAAC AATTACTACT ACGGATGCTC AAACTTCTAC TGATTCAACG ATTACTACTA CAGATTCAAC

321'  TACAGTCAAG ACTGAGCCTC CCGTCTCAGA GGGCAACAAC CCAGTGGAAG AGAACAACGA AAACGGAGTA GGGAAAGACG
      ******* ** ********** ********** * ******** ********** ********** ********** **********
321"  TACAGTCGAG ACTGAGCCTC CCGTCTCAGA GCGCAACAAC CCAGTGGAAG AGAACAACGA AAACGGAGTA GGGAAAGACG

401'  ATGAAAATCT TTTTCCTCTC GTTGTCAAGG ATAAGTCACT GCTCCAGTTA ATGGGCTATG CAGCTTAG
      ********** ********** ********** ********** ********** ********** ********
401"  ATGAAAATCT TTTTCCTCTC GTTGTCAAGG ATAAGTCACT GCTCCAGTTA ATGGGCTATG CAGCTTAG
```

B

```
1'  MNSTACKYYT ERTLGWMLNN KTIVFLSLLS FCLFVSTLAL AGQRNRLTAE VDDLRHRLTT SSVLETTTPI NVDTTTTTEG
    ********** ********** ********** ********** ********** ********** ********** **********
1"  MNSTACKYYT ERTLGWMLNN KTIVFLSLLS FCLFVSTLAL AGQRNRLTAE VDDLRHRLTT SSVLETTTPI NVDTTTTTEG

81'  QTTTDSTITT TDAQTSTDST ITTTDSTTVK TEPPVSEGNN PVEENKENGV GKDDENLFPL VVKDKSLLQL MGYAA
     ********** ********** *********. ******* ** ********** ********** ********** *****
81"  QTTTDSTITT TDAQTSTDST ITTTDSTTVE TEPPVSERNN PVEENKENGV GKDDENLFPL VVKDKSLLQL MGYAA
```

C

```
  1' ATGAATTCAA CCGCGTGCAA GTATTACACG GAAAGAACTC TGGGTTGGAT CTTGAACAAC AAAACGATAG TGTTTCTTTC
     ********** ********** ********** ********** ********** ********** ********** **********
  1" ATGAATTCAA CCGCGTGCAA GTATTACACG GAAAGAACTC TGGGTTGGAT CTTGAACAAC AAAACGATAG TGTTTCTTTC

 81' ATTACTGTCA TTCTGTTTGT TTGTTTCGAC GTTAGCGTTG GCCGCGCAGA CGAATCGGCT CACGGCCGAG GTGGACGATC
     ********** ********** ********** ********** ********** ********** ********** **********
 81" ATTACTGTCA TTCTGTTTGT TTGTTTCGAC GTTAGCGTTG GCCGCGCAGA CGAATCGGCT CACGGCCGAG GTGGACGATC

161' TCAGCCACCG TTTGACCACG TCTTCTGTTC TGGAAACTAC AACACCAATC AACGTAGACA CAACAACTAC TACAGAAGAT
     ********** ********** ********** ********** ********** ********** ********** **********
161" TCAGCCACCG TTTGACCACG TCTTCTGTTC TGGAAACTAC AACACCAATC AACGTAGACA CAACAACTAC TACAGAAGAT

241' TCAACTACAG TCAAGACTGA GCCTCCCGTC TCAGAGGGCA ACAACCCAGT CGAAGAGAAC AAGGAAAACG GAGTAGGGAA
     ********** ** ******* ********** ****** *** ********** ********** ********** **********
241" TCAACTACAG TCGAGACTGA GCCTCCCGTC TCAGAGCGCA ACAACCCAGT CGAAGAGAAC AAGGAAAACG GAGTAGGGAA

321' AGACGATGAA AATCTTTTTC CTCTCGTTGT CAAGGATAAG TCACTGCTCC AGTTAATGGG CTATGCAGCT TAG
     ********** ********** ********** ********** ********** ********** ********** ***
321" AGACGATGAA AATCTTTTTC CTCTCGTTGT CAAGGATAAG TCACTGCTCC AGTTAATGGG CTATGCAGCT TAG
```

D

```
  1' MNSTACKYYT ERTLGWMLNN KTIVFLSLLS FCLFVSTLAL AGQRNRLTAE VDDLRHRLTT SSVLETTTPI NVDTTTTTED
     ********** ********** ********** ********** ********** ********** ********** **********
  1" MNSTACKYYT ERTLGWMLNN KTIVFLSLLS FCLFVSTLAL AGQRNRLTAE VDDLRHRLTT SSVLETTTPI NVDTTTTTED

 81' STTVKTEPPV SEGNNPVEEN KENGVGKDDE NLFPLVVKDK SLLQLMGYAA
     ****.***** ** ******* ********** ********** **********
 81" STTVETEPPV SERNNPVEEN KENGVGKDDE NLFPLVVKDK SLLQLMGYAA
```

Figure 2.2 Sequence comparison of the *nsd-1* mutant genes from resistant (p50T) and susceptible (J150) strains

(A, B) Alignment of nucleotide (A) and deduced amino acid sequences (B) of non-spliced form of the *nsd-1* mutant gene from resistant (p50T) and susceptible (J150) strains. (C, D) Alignment of nucleotide (C) and deduced amino acid sequences (D) of spliced form of the *nsd-1* mutant gene from resistant (p50T) and susceptible (J150) strains. The red characters indicate the nucleotide and amino acid substitutions between resistant (p50T) and susceptible (J150) strains.

2.3.3 Expression of the *nsd-1* candidate gene

In RT-PCR using total RNA isolated from 8 different tissues, the expression of the *nsd-1* candidate gene was detected only in the midgut (Fig. 2.3A). The midgut specific expression of this gene was consistent with the unique characteristic that BmDNV-1 is able to infect only midgut cells (Kawase and Kurstak, 1991). Also, I examined the expression pattern during the developmental stages and observed that the candidate gene was detected in the later stages of embryo and throughout the adult stages (Fig. 2.3B). The ubiquitous expression during the developmental stages suggests that this gene not only serves for densovirus infection but also plays other roles in the midgut including the digestion and absorption processes.

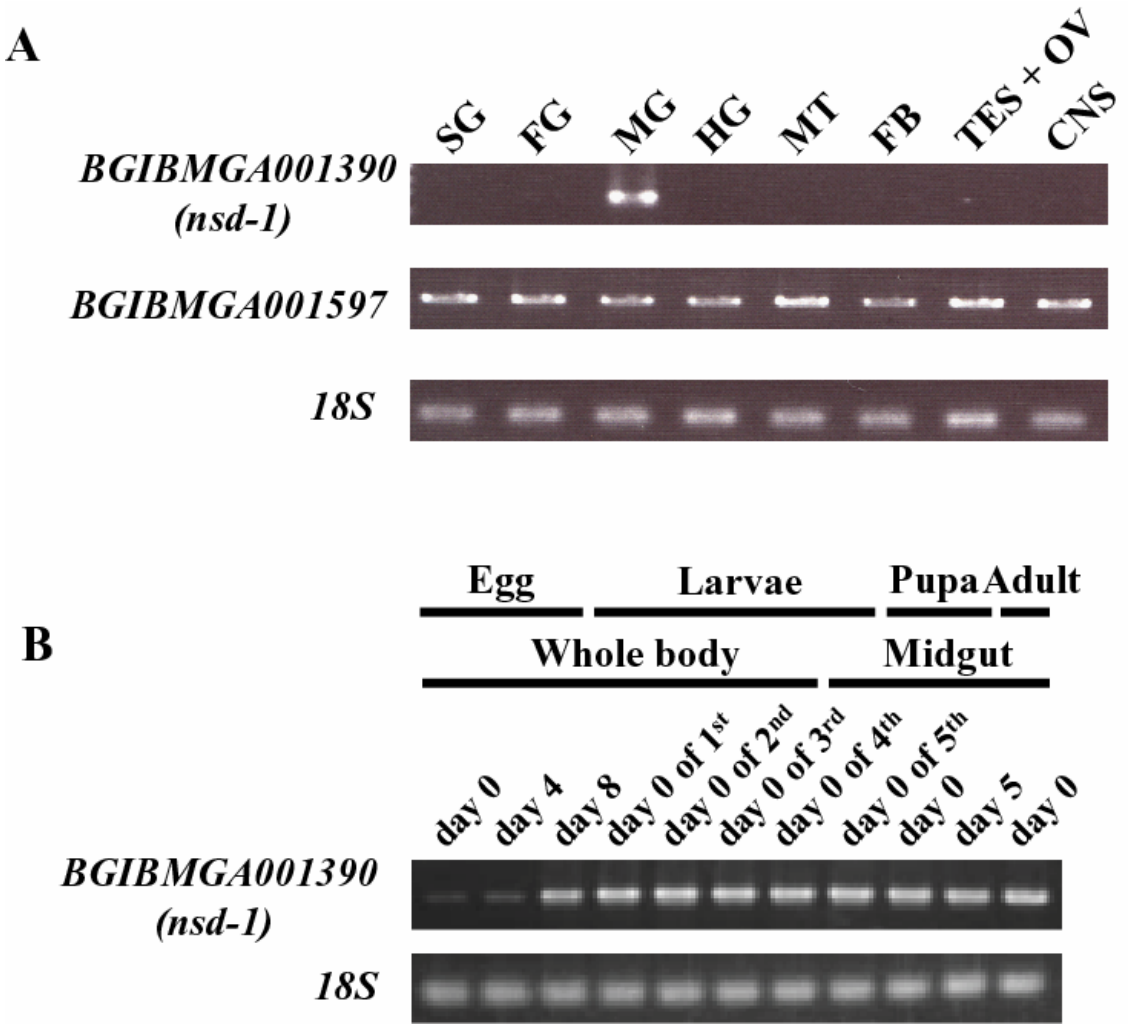

Figure 2.3 Expression analysis of the *nsd-1* candidate gene

(A) RT-PCR analysis of the *nsd-1* candidate gene in 8 tissues of wild-type strain p50T. Primer sets are for BGIBMGA001390, BGIBMGA001597, and ribosomal *18S*, a positive control. Lane 1, silk gland (SG); 2, foregut (FG); 3, midgut (MG); 4, hindgut (HG); 5, Malpighian tubule (MT); 6, fat body (FB); 7, testis plus ovary (TES + OV); 8, central nervous system (CNS). (B) RT-PCR analysis of stage-specific expression of the *nsd-1* mutant gene in wild-type strain p50T. Lanes 1–3, egg, day 0, 4 and 8; Lanes 4–7, whole body, day 0 of first to fourth instar larva; Lane 8, midgut, day 0 of fifth instar larva; Lanes 9 and 10, pupal gut, day 0 and 5; Lane 11, adult gut, day 0.

2.3.4 Genomic structure and deduced amino acid sequence of the *nsd-1* candidate gene

To determine the full length cDNA sequence of the *nsd-1* candidate gene, I performed 5'- and 3'-RACE using the cDNA prepared from the midgut from day 0 fifth instar larvae. DNA sequencing showed two alternatively spliced variants of the *nsd-1* candidate gene. The complete cDNA sequence of one of the variants, the non-spliced form, was 1016 bp-long and this form potentially encodes a protein of 155 amino acids and contains no intron (Fig. 2.4). On the other hand, the ORF of another variant, the spliced form, was 888 bp-long and potentially encodes a protein of 130 amino acids. This variant consists of two exons and one intron (Fig. 2.4). Both of these two variants were found in the *B. mori* EST database (fmgV3h04; the non-spliced form and fmgV37b04; the spliced form), suggesting that both forms are actually expressed in the midgut. Sequencing of the PCR products also showed that the major isoform was the non-spliced form, because the cloning frequency of the non-spliced form was 2.5 times higher than that of the spliced form.

By NCBI-blastp search against the NCBI protein database, the deduced amino acid sequence of the cDNA sequence of the *nsd-1* candidate did not show homology to any known proteins. The topology and motif prediction showed that this protein has one putative transmembrane domain and a mucin-like domain containing threonine and serine rich sequences (Fig. 2.5).

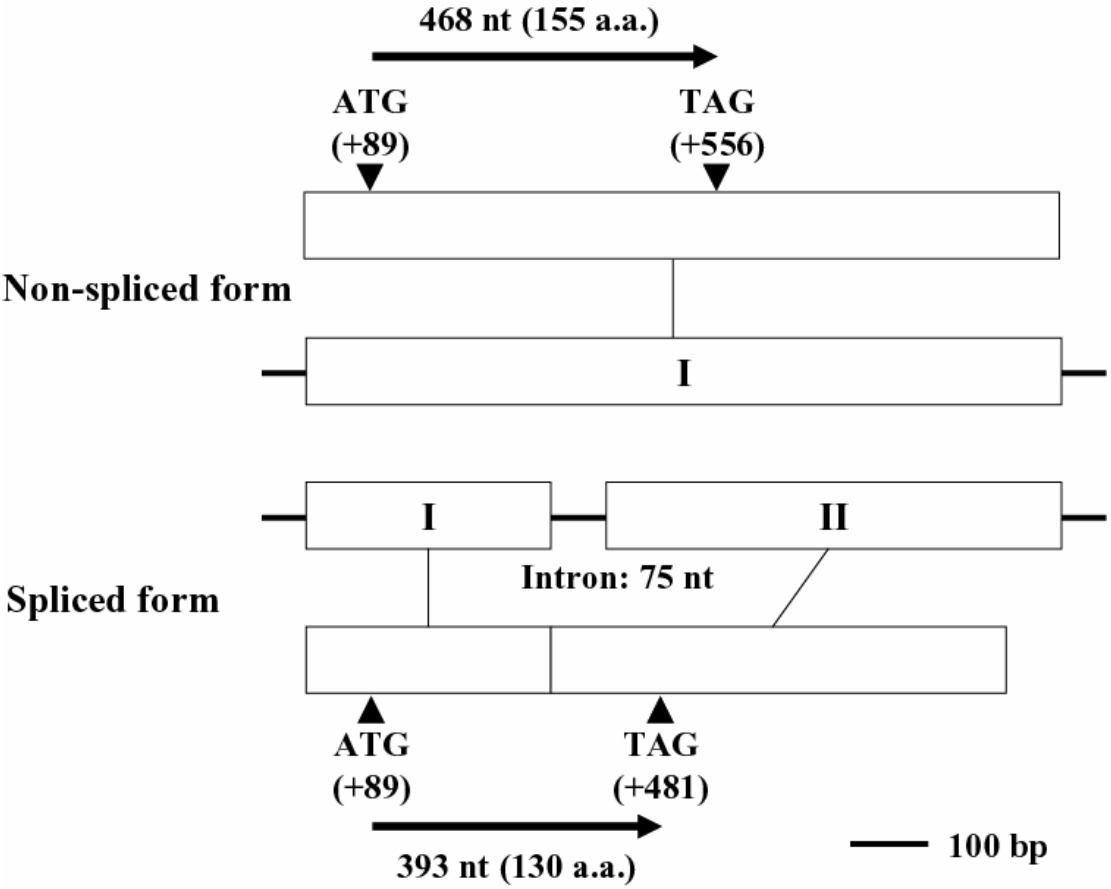

Figure 2.4 Schematic structure of the *nsd-1* candidate gene

Genomic and cDNA structures of the *nsd-1* gene of the wild-type strain p50T. The upper figure indicates the non-spliced form of *nsd-1*, and the lower indicates the spliced form of *nsd-1*. The arrowheads show the start and stop codons. The arrows indicate the coding region.

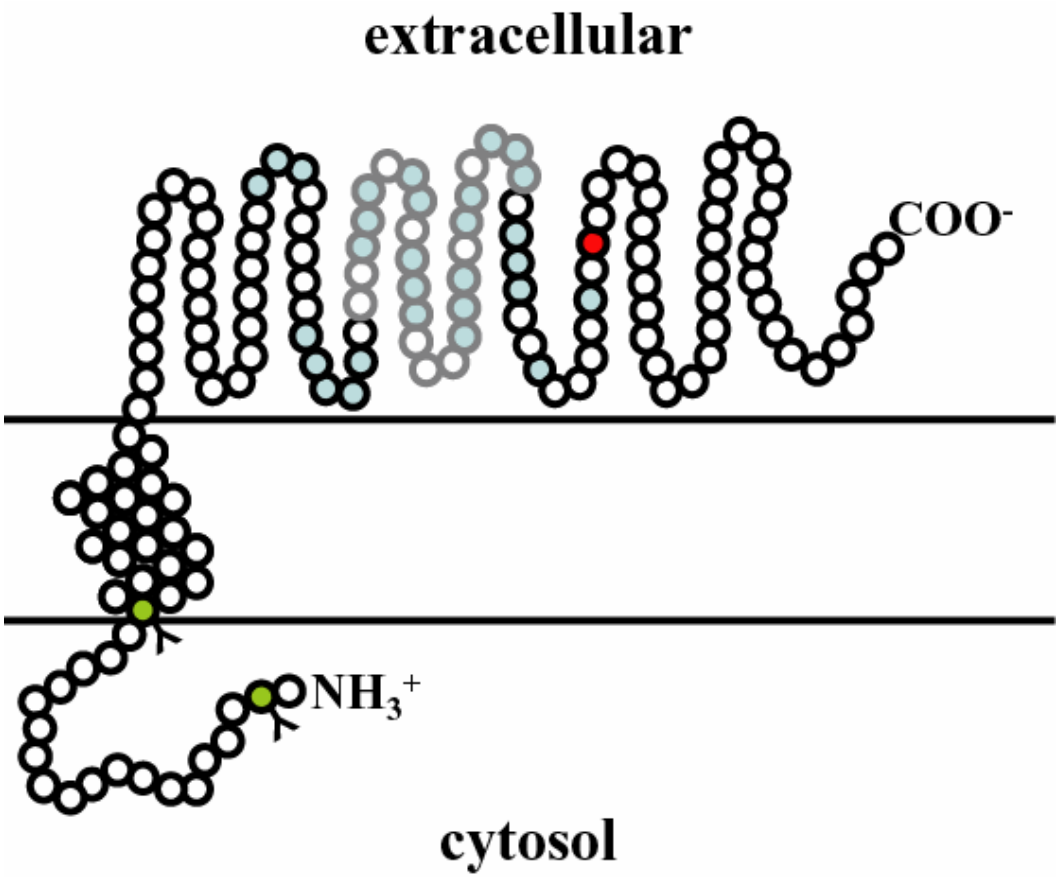

Figure 2.5 Hypothetical secondary structure of NSD-1

The secondary structure of NSD-1 was predicted by SOSUI. The spliced form of NSD-1 lacks the gray region. The red circle indicates the arginine residue which might be crucial for BmDNV-1 infection. The blue and green circles indicate the putative O-linked glycosylation and N-linked glycosylation sites ("Y" marks), respectively.

2.3.5 Comparison of SNPs in *nsd-1* among resistant and susceptible strains

I performed comparative studies of SNPs observed in 11 resistant and 13 susceptible strains. DNA sequencing showed that arginine residue at 118 of non-spliced form and 93 of spliced form of NSD-1 was conserved in all of the susceptible strains. The topology analysis by SOSUI indicated that the position of this residue was located in the extracellular side suggesting that this arginine residue might be critical for susceptible infection to BmDNV-1 (Table 2.3).

Table 2.3. Comparison of SNPs between resistant and susceptible strains.

11 resistant strains		
strain	position	
	110 aa (85 aa)*	118 aa (93 aa)*
B	K	G
p50T	K	G
C108T	K	G
C124	K	G
No. 104	K	P
No. 115	K	P
No. 138	K	G
No. 141	K	P
No. 603	K	P
No. 902	K	P
No. 910	K	P

13 susceptible strains		
strain	position	
	110 aa (85 aa)*	118 aa (93 aa)*
J02	E	**R**
J124	E	**R**
J150	E	**R**
No. 101	E	**R**
No. 102	E	**R**
No. 122	K	**R**
No. 123	K	**R**
No. 126	E	**R**
No. 133	E	**R**
No. 142	K	**R**
No. 144	E	**R**
No. 146	E	**R**
No. 918	K	**R**

*The number indicates the position of amino acid substitution of non-spliced form.
The number shown in parentheses indicates the position of amino acid substitution of spliced form.

2.3.6 Western blot analysis of NSD-1

To examine the biochemical properties of NSD-1, I generated BmN cells stably expressing His-tagged NSD-1. Western blot analysis using Penta-His antibody showed that broad signals were observed at 28-40 kDa and their patterns were quite similar to those detected when anti-NSD-1 antibody was used (Lanes 1-4, 9-12; Fig. 2.6). Also, I detected NSD-1 expression by Western blot of the extract from larval midgut membrane with anti-NSD-1 antibody (Lane 6; Fig. 2.6). These results suggest that the anti-NSD-1 antibody actually recognizes NSD-1 itself. According to the NSD-1 sequence, the mass of this protein is 17 kDa in the non-spliced form and 14 kDa in the spliced form, indicating that NSD-1 has some modifications including N- and O-linked glycosylations in BmN cells and larval midgut as predicted by the motif analysis (Fig. 2.6). In addition, I found that the signal patterns were different between non-spliced and spliced forms. The signals of non-spliced form were weak and broad compared to those of spliced form. This difference might be attributable to the fact that the non-spliced form of NSD-1 has more O-linked glycosylation sites than the spliced one (Fig. 2.6).

Also, I observed a marked difference of the signal patterns in resistant (p50T) and susceptible (J150) strain. The signals of NSD-1 from the resistant strain were smaller than those from the susceptible strain. Western blot analysis using the point mutated constructs clearly showed that the difference observed in resistant and susceptible strains was determined by a single amino acid substitution at residues 110 (K110E) of non-spliced form or 85 (K85E) of spliced form.

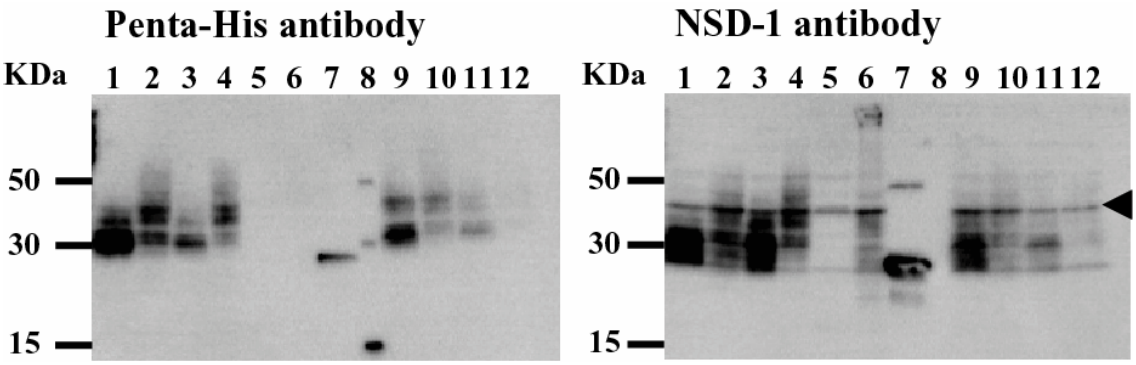

Figure 2.6 Western blot of NSD-1

The membrane proteins were extracted from BmN cells stably expressing His-tagged NSD-1 and midgut of *B. mori* larvae (resistant strain p50T), and analyzed by Western blot. The primary antibodies used were Penta-His antibody and NSD-1 antibody. Lane 1, NSD-1-G93R-sp (G93R); 2, NSD-1-K85E-sp (K85E); 3, NSD-1-Res-sp (resistant strain-p50T); 4, NSD-1-Sus-sp (susceptible strain-J150); 5, pIZ/V5-His vector (control); 6, midgut of *B. mori* larvae (resistant strain p50T); 7, NSD-1 antigen; 8, 6 x His Protein Ladder; 9, NSD-1-G118R-nonsp (G118R); 10, NSD-1-K110E-nonsp (K110); 11, NSD-1-Res-nonsp (resistant strain-p50T); 12, NSD-1-Sus-nonsp (susceptible strain-J150). The arrowhead indicates the non-specific band.

2.3.7 Modification of NSD-1 with N- and O-linked glycans

To examine whether NSD-1 is glycosylated in BmN cells, I treated NSD-1 with PNGase F, which cleaves N-linked glycans from proteins. By this treatment, an apparent signal of approximately 30 kDa was observed compared to when PNGase F was not treated (Lanes 1-4, Fig. 2.7), suggesting that NSD-1 is modified with N-linked glycans. Next, I examined O-linked glycosylation of NSD-1 by the treatment with O-glycosidase. As shown in Fig. 2.7 (Lanes 6-9), the treatment with O-glycosidase resulted in a reduction in the molecular masses of NSD-1, suggesting that NSD-1 has O-linked glycans. From these results, I conclude that NSD-1 is a glycosylated protein with N- and O-linked glycans.

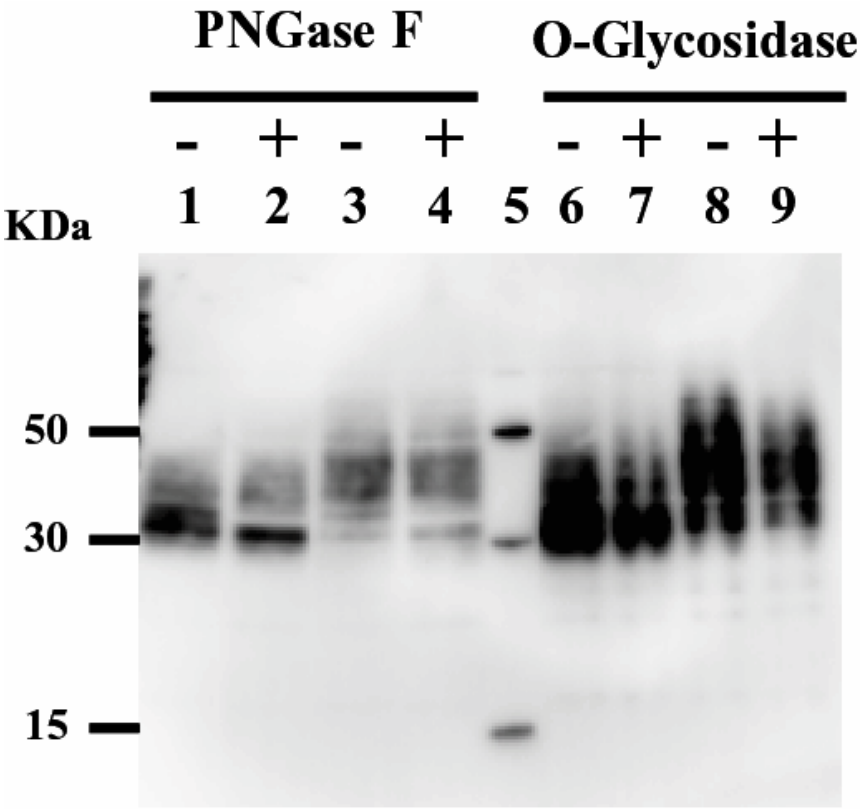

Figure 2.7 N- and O-linked glycosylation of NSD-1

The membrane fractions were prepared from BmN cells stably expressing NSD-1-Res-sp (resistant strain-p50T) and NSD-1-Sus-sp (susceptible strain-J150). The extracted membrane proteins were treated with or without glycosidase to remove N- or O-linked glycans. Detection of NSD-1 was performed by Western blot using Penta-His antibody as a primary antibody. Lanes 1, 2, 6, and 7, NSD-1-Res-sp; 3, 4, 8, and 9, NSD-1-Sus-sp. Lanes 1-4, with (+) or without (-) PNGase F; 5, 6 x His Protein Ladder; 6-9, with (+) or without (-) O-glycosidase.

2.3.8 Expression and localization of NSD-1 in larval midgut

Next, I examined the expression and localization of NSD-1 in larval midgut by anti-NSD-1 antibody. Immunohistochemical experiments showed that strong signals for NSD-1 were observed in the columnar cells of midgut epithelium (Fig. 2.8). This result strongly suggests that NSD-1 may play an important role in entry or binding of BmDNV-1 to the columnar cells of midgut epithelium.

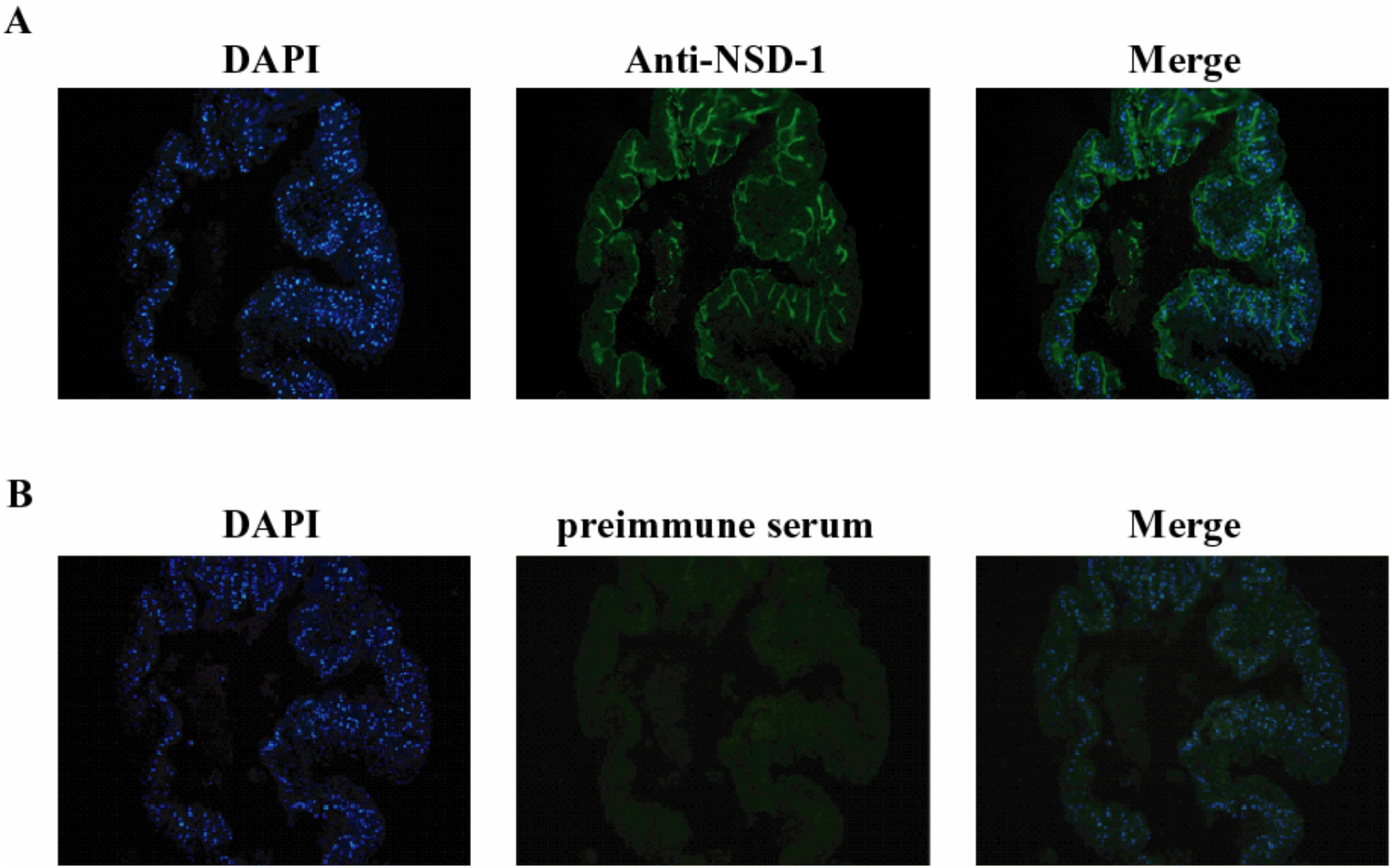
A
DAPI
Anti-NSD-1
Merge
B
DAPI
preimmune serum
Merge

Figure 2.8 Immunohistochemical analysis of NSD-1 protein in the larval midgut

(A) Immunofluorescence visualization of NSD-1. (B) Control experiments using preimmune serum. Sections were incubated with anti-NSD-1 antibody or preimmune serum followed by the secondary antibody labeled with AlexaFluor488 (green) and counterstained with DAPI.

2.4 Discussion

In this chapter, I performed positional cloning of the *nsd-1* mutant gene based on *B. mori* genome information, and identified a novel mucin-like gene as the candidate. This gene potentially encodes a protein with one putative transmembrane domain. Also, sequence analysis and biochemical experiments revealed that this protein has two N-linked glycosylation sites in the intracellular region and many O-linked glycosylation sites in the extracellular mucin-like domain (Figs. 2.5 and 2.7). Comparative studies of SNPs observed in this gene from 11 resistant and 13 susceptible strains strongly suggested that a single amino acid substitution might be crucial for susceptible infection with BmDNV-1.

RT-PCR analysis clearly showed that the *nsd-1* candidate was expressed only in the midgut (Fig. 2.3). Also, immunohistochemical observation revealed that NSD-1 protein was expressed on the surface of the columnar cells in larval midgut epithelium (Figs. 2.8). This observation is consistent with the unique characteristic that BmDNV-1 is able to infect only midgut columnar cells (Kawase and Kurstak, 1991). Taken together, these results strongly suggest that the isolated gene is *nsd-1*, and the NSD-1 protein may play an important role in entry or binding of BmDNV-1 to the columnar cells. To verify whether the candidate gene is responsible for virus resistance, I am attempting to generate the transgenic silkworm of a resistant strain transformed with the susceptible type of *nsd-1*.

DNA sequencing of *nsd-1* from resistant and susceptible strains showed that arginine residue at 118 of NSD-1 was conserved in all of the susceptible strains, but substituted by glycine or proline in resistant strains (Table 2.3). Topology analysis of NSD-1 suggested that this residue is located in the extracellular region, indicating that this

residue might infect with BmDNV-1 directly. Infection mechanisms have been reported in canine parvovirus (CPV) and feline panleukopenia virus (FPV) (Palermo et al., 2003). Their infection is caused by binding of the virus to the transferrin receptor of their hosts. The relationship between them is very specific; the combination of residues within a specific region of the viral capsid and several residues in the apical domain of the feline and canine transferrin receptors control host-specific binding and cell infection of CPV and FPV (Palermo et al., 2003). In the case of BmDNV-1 infection to *B. mori*, the charge on the arginine residue of susceptible NSD-1 may play an important role for the binding to the raised region of capsid protein of BmDNV-1. It is still not clear whether the NSD-1 protein can bind to BmDNV-1 or not, and how BmDNV-1 interacts with NSD-1. Further biochemical studies using recombinant proteins and/or transformed cell lines will determine the binding and the recognition sites of BmDNV-1 and NSD-1.

Nid-1 is another resistant gene against BmDNV-1 (Eguchi et al., 2007). The study of BmDNV-1 infection using the silkworm with midgut mosaicism in infected ($+^{Nid\text{-}1}/+^{Nid\text{-}1}$) and noninfected (*Nid-1*/$+^{Nid\text{-}1}$) areas showed that degraded columnar cells were observed only in the infected area (Abe et al., 1990). On the other hand, the noninfected epithelium of the mosaic midgut is composed of a large number of columnar cells arranged tightly with a few goblet cells among them. According to the histological features of the mosaic midgut, the factor, if any, may not be exudative, but works in the cell *in situ*. Although *Nid-1* mutation has been mapped to the classical map, the responsible gene has not been identified. Therefore, it would be of great importance to identify the gene corresponding to *Nid-1*. Interestingly, *Nid-1* has been shown to be genetically epistatic to $+^{nsd\text{-}1}$ (Abe et al., 1987). The determination of the relationship between *Nid-1* and *nsd-1* will contribute to analysis of the infection mechanism of

densoviruses.

General Discussion

A number of viruses, including nucleopolyhedrovirus (NPV), cypovirus (CPV), infectious flacherie virus (IFV), and densovirus (DNV) are known to infect the silkworm *Bombyx mori*. Serious damage to sericultures can be attributed directly to silkworm diseases, rather than to unfavorable weather conditions. Therefore, the use of silkworm strains resistant to diseases is a prerequisite for more effective disease prevention. Some silkworm strains can resist a high density of one or more kinds of virus, but they will become infected when the virus that they ingest exceeds a certain point. On the other hand, there are some strains showing absolute resistance to BmDNVs regardless of the amount of viruses they ingest.

The resistance of *B. mori* to BmDNVs is of the "nonsusceptible" type and appears to be a unique case in the silkworm, as compared with other animals and plants. It is still unknown how the resistance genes control the resistance against BmDNVs. Although silkworm susceptibility to viruses, with the exception of BmDNVs, varies greatly depending upon the developmental stage and rearing conditions, such as temperature and food quality, the resistance is generally controlled by polygenes. Nevertheless, several reports have indicated that the major factor in insect resistance to viruses, including IFV, CPV, and NPV, is encoded by a single major gene (Watanabe et al., 1986; Watanabe, 2002). Identification of the virus-resistant genes and their products will provide a better understanding of the mechanisms of viral infection and insights into the molecule interactions between microbes and host animals. In this dissertation, I performed the isolation and characterization of two mutant genes *nsd-1* and *nsd-2*, which control the infectivity of BmDNV-1, and BmDNV-2.

In the Chapter 1, I attempted to identify the *nsd-2* mutant gene by positional cloning, and successfully cloned *nsd-2*, which potentially encodes a putative amino acid transporter. Also, I found that a part of *nsd-2* corresponding to 9 out of 12 predicted transmembrane domains is deleted in the resistant strain. Expression of a wild type transgene in the midgut by germline transformation restores susceptibility to BmDNV-2, clearly showing that the defective membrane protein is responsible for the resistance. This is the first report of the isolation of the mutant gene that causes absolute resistance to a virus in insects.

The function of NSD-2 as an amino acid transporter

The cDNA sequence of the susceptible type of *nsd-2* revealed that NSD-2 shows high homology with two amino acid transporters of *M. sexta* (Catagne et al., 1998; Feldman et al., 2000). These amino acid transporters have function as a the K^+-coupled amino acid transporter which is a Lepidopteran neutral amino acid transporter belonging to the neurotransmitter sodium symporter (Catagne et al., 1998), and the cation-anion-activated amino acid transporter/channel which acts as Cl^--independent, and Na^+- or K^+-activated nutrient amino acid transporter (Feldman et al., 2000). Whether NSD-2 actually functions as an amino acid transporter or not is still unknown. Interestingly, the resistant strain possessing a large deletion of this transporter gene grows normally under normal conditions, suggesting that *nsd-2* is not indispensable for the silkworm. During the positional cloning, at the genomic locus near *nsd-2*, I found another gene that also encodes a putative transporter, but has no relationship to viral resistance (data not shown). The deduced amino acid sequence from this gene shows a relatively high sequence identity (69%) with NSD-2. The product of this gene might

function as an amino acid transporter instead of NSD-2. To verify this hypothesis, it is required to determine the function of this membrane protein as an amino acid transporter.

The amino acid transporter as a virus receptor

In murine leukemia virus, which belongs to Retroviridae, infection begins by binding of the virus envelope to a murine cationic amino acid transporter (Albritton et al., 1989). The relationship between the virus and the transporter is very specific. Other leukemia viruses, for example human leukemia virus, cannot recognize the murine transporter nor can the murine leukemia virus bind to the human transporter (Yoshimoto et al., 1991; Albritton et al., 1993) although the human cationic amino acid transporter has high homology with that of murine (87%). For this mechanism, it is reported that specific amino acids both on the viral envelope protein and on the exposed domain of the transporter are important for binding of the two (Mackrell et al., 1996; Bae et al., 1997; Qian et al., 2003). BmDNV-2 is a non-enveloped virus and differs from retroviruses at many points, including genome structure, genome size, virus surface structure and more. In this regard, it would be of great interest to determine the recognition sites of BmDNV-2 and NSD-2.

The relationship between BmDNV-2 and BmDNV-Z

BmDNV-2 (Yamanashi isolate) and -Z (Zhenjiang isolate) are classified into the parvo-like virus, but their virulence and the symptoms of infection are different. BmDNV-2 almost exclusively infects the columnar cells of midgut epithelium, while BmDNV-Z can infect the columnar cells of midgut epithelium during the early stage of

infection and infect the goblet cells during the late stage of infection (Wang et al., 2007). Comparison of the complete genome sequence between BmDNV-2 and BmDNV-Z showed an identity of 98.4% in VD1 and 97.7% in VD2 (Wang et al., 2007). Also, it has been shown that the resistance of BmDNV-Z is determined by a single gene, which was mapped on chromosome 15 (Li et al., 2006). By cloning *nsd-Z*, I will be able to compare the infection mechanisms of these two closely related viruses.

In the Chapter 2, I described the isolation of *nsd-1* candidate gene by positional cloning and the functional analysis of this gene using biochemical and immunohistochemical techniques.

Is the candidate gene responsible for the resistance to BmDNV-1?

By positional cloning, I succeeded to identify a novel mucin-like gene as the *nsd-1* candidate. The deduced amino acid sequence from this gene revealed that NSD-1 is a membrane protein which encompasses one putative transmembrane domain. Sequencing of *nsd-1* in some susceptible and resistant strains showed that one amino acid substitution in NSD-1 might be crucial for susceptible infection to BmDNV-1. Also, I examined the expression and localization of NSD-1 in larval midgut by immunohistochemical analysis, and found that this protein was expressed in the columnar cells of midgut epithelium. These genetic and immunohistochemical analyses strongly suggest that the isolated gene is the *nsd-1* mutant gene itself. However, I do not have any evidence directly showing that the isolated gene corresponds to the *nsd-1* mutant gene. Therefore, as a next approach, to verify whether the candidate gene is responsible for virus resistance, I am now attempting to generate the transgenic

silkworm of a resistant strain transformed with the susceptible type of *nsd-1*.

The relationship between *Nid-1*and *nsd-1*

The resistance of *B. mori* larvae to BmDNV-1 was controlled by two genes, *Nid-1* and *nsd-1*. In this dissertation, I successfully cloned the candidate gene by map-based cloning. Immunohistochemical experiments showed that strong signals for NSD-1 were observed in the columnar cells of midgut epithelium (Fig. 2.8), suggesting that NSD-1 may have a function as a virus receptor. On the other hand, *Nid-1* is not yet identified. Genetic experiments revealed that *Nid-1* is epistatic to $+^{nsd-1}$(Abe et al., 1987). These results suggest that the *Nid-1* gene product may not be exudative, but works on the cell surface or in the cell. To know how *Nid-1* controls the resistance to BmDNV-1, it is necessary to identify the *Nid-1* mutant gene. I have also been trying to isolate this gene by positional cloning, and succeeded to narrow the *Nid-1* linked region to about 400 kb (data not shown). Now, collaborators in National Institute of Agrobiological Sciences (NIAS) are continuing to isolate this mutant gene, and succeeded to narrow the *Nid-1* linked region to less than 100 kb (K. Kadono-Okuda and K. Kidokoro, personal communications). In near future, the *Nid-1* gene will be cloned and the relationship between *nsd-1* and *Nid-1*will be understood at the molecular level.

Infection mechanisms of densoviruses

In parvovirus, there are many reports on the factor related the virus infection, for example, their receptors on the host cell surface and several critical capsid residues. Human parvovirus B19, the most studied parvovirus, is known to utilize three receptors, erythroid P antigen, α5β1 integrin, and Ku80 autoantigen (Brown et al., 1993;

Weigel-Kelley et al., 2003; Munakata et al., 2005). Although many studies on host ranges or tissue specificities of densoviruses have been done, the host and/or virus factors controlling host and tissue specificity are still unknown. NSD-1 and NSD-2 are the first molecules that determine the host specificity in densovirus infection. The cell surface molecules might be an important factor for virus infection like human parvovirus. Topology analysis indicated that both NSD-1 and NSD-2 are membrane proteins (Figs. 1.5 and 2.5), suggesting that they might function as cell surface receptors for BmDNVs. NSD-2 has two putative N-glycosylation sites (Fig. 1.5), while NSD-1 has two N-linked glycosylation sites in the intracellular region and several clusters of O-linked glycosylation sites in the extracellular mucin-like domain (Figs. 2.5 and 2.7). Studies on parvovirus showed that modification of its receptor with N-glycans is important for viral binding to the receptor (Parker et al., 2000, Cotmore and Tattersall., 2007). Further experiments are required to determine whether N- and/or O-glycans are critical for DNV binding to NSD-1 and NSD-2.

In vitro studies using cultured cells have largely contributed to the understanding of receptor biochemistry and pharmacology. Previous studies showed that cell lines that AeDNV and JcDNV can infect are available (Jousset, et al., 1993; Li, et al., 1995). This is presumably because these DNVs have a broad tissue tropism (Jousset, et al., 1993; Li, et al., 1996). Using the cultured cells, several biochemical studies of these viruses have been performed (Ward et al., 2001, Afanasiev and Carlson, 2000, Shirk et al., 2007).

In *B. mori*, however, cell lines that BmDNVs can infect have not been discovered. This is one of the reasons why infection mechanisms of BmDNVs are still not answered. Most of *B. mori* cell lines are originated from ovary and embryo, and no cell line generated from midgut cells has been reported. To overcome this problem, I tried to

generate BmN4 cells stably expressing *nsd-1* and *nsd-2*, and successfully isolated recombinant cells producing NSD-1 (Chapter 2) and NSD-2 (data not shown). Using these cells, I am now preparing to perform biochemical experiments for analyzing interaction between BmDNVs and their putative receptors. This approach will provide novel information on molecular mechanisms of BmDNV infection.

Concluding remarks

In this dissertation, I succeeded to identify two BmDNV resistant genes, *nsd-1* and *nsd*-2 by positional cloning. The products of these genes were the membrane protein expressed only in the midgut, indicating that these proteins function as cell-surface receptors for BmDNVs. In Densovirinae, the factors that determine host and tissue specificities have not been identified to date. The present study is the first report on identification of the host genes that cause absolute resistance to a virus in insects. Although the genes responsible for the virus resistance were isolated, it is still not clear how BmDNVs interact with respective membrane proteins. Examining their interactions by biochemical and pharmacological techniques will give new insights into the molecular mechanism of insect virus infection.

Acknowledgments

I am very much indebted to Professor Dr. Toru Shimada, Associate Professor Dr. Susumu Katsuma, and Assistant Professor Dr. Takaaki Daimon for guiding me to the field of insect genetics, and their strong support and encouragement during the course of this study.

I am grateful to Dr. Keiko Kadono-Okuda, Dr. Kazuei Mita, Dr, Kimiko Yamamoto, Dr. Kurako Kidokoro, Dr. Andrew Kalyebi, Dr. Toshiki Tamura, Dr. Sezutsu Hideki, Dr. Keiro Uchino, Dr. Isao Kobayashi, Dr. Ryokitsu Eguchi, Dr. Wajiro Hara, Ms. Junko Nohata, Mr. Shunichi Sasanuma, Ms. Motoe Sasanuma, and Ms. Reiko Komatsuzaki for their help with experiments and stimulating discussions on the *Bombyx* and densovirus research.

I wish to express thanks to all members of the Division of Insect Sciences of NIAS and the Laboratory of Insect Genetics and Bioscience of The University of Tokyo.

References

Abe, H., Watanabe, H., and Eguchi, R. (1987) Genetical relationship between nonsusceptibilities of the silkworm, Bombyx mori, to two densonucleosis viruses. J. Seric. Sci. Jpn. **56**, 443-444. (In Japanese).

Abe, H., Kobayashi, M., Watanabe, H. (1990) Mosaic infection with a densonucleosis virus in the midgut epithelium of the silkworm, Bombyx mori. *J. Invertebr. Pathol*. **55**,112-117.

Abe, H., Shimada, T., Kobayashi, K., Maeda, S., Yokoyama, T., Oshiki, T., Kobayashi, M. (1993) Detection of densonucleosis virus in the silkworm, Bombyx mori, from fecal specimens by a polymerase chain reaction. *J Seric Sci Jpn* **62**, 376-381 (in Japanese with English abstract).

Abe, H., Harada, T., Kanehara, M., Shimada, T., Ohbayashi, F., Oshiki, T. (1998) Genetic mapping of RAPD markers linked to the densonucleosis refractoriness gene, nsd-1, in the silkworm, *Bombyx mori*. *Genes Genet Syst.* **73**, 237-242.

Abe, H., Sugasaki, T., Kanehara, M., Shimada, T., Gomi, S. J., Ohbayashi, F., Oshiki, T. (2000) Identification and genetic mapping of RAPD markers linked to the densonucleosis refractoriness gene, *nsd-2*, in the silkworm, *Bombyx mori*. *Genes Genet Syst* **75**, 93-96.

Afanasiev, B. and Carlson, J. (2000) Densovirinae as gene transfer vehicles. *Contrib Microbiol* **4**, 33-58

Albritton, L. M., Tseng, L., Scadden, D., Cunningham, J. M. (1989) A putative murine ecotropic retrovirus receptor gene encodes a multiple membrane-spanning protein

and confers susceptibility to virus infection. *Cell* **57**, 659-666.

Albritton, L. M., Kim, J. W., Tseng, L., Cunningham, J. M. (1993) Envelope-binding domain in the cationic amino acid transporter determines the host range of ecotropic murine retroviruses. *J Virol.* **67**, 2091-2096.

Asser-Kaiser, S., Fritsch, E., Undorf-Spahn, K., Kienzle, J., Eberle, K. E., Gund, N. A., Reineke, A., Zebitz, C. P., Heckel, D. G., Huber, J., Jehle, J. A. (2007) Rapid emergence of Baculovirus resistance in codling moth due to dominant, sex-linked inheritance. *Science* **317**, 1916-1918.

Bae, Y., Kingsman, S. M., Kingsman, A. J. (1997) Functional dissection of the Moloney murine leukemia virus envelope protein gp70. *J Virol.* **71**, 2092-2099.

Bando, H., Choi, H., Ito, Y., Kawase, S. (1990) Terminal structure of a Densovirus implies a hairpin transfer replication which is similar to the model for AAV. *Virology* **179**, 57-63.

Bando, H., Choi, H., Ito, Y., Nakagaki, M., Kawase, S. (1992) Structural analysis on the single-stranded genomic DNAs of the virus newly isolated from silkworm: the DNA molecules share a common terminal sequence. *Arch Virol*. **124**, 187-193.

Bando, H., Hayakawa, T., Asano, S., Sahara, K., Nakagaki, M., Iizuka, T. (1995) Analysis of the genetic information of a DNA segment of a new virus from silkworm. *Arch Virol.* **140**, 1147-1155.

Bergoin, M. and Tijssen, P. (2000) Molecular biology of Densovirinae. *Contrib Microbiol* **4**, 12-32.

Bradford, M. M. (1976) A rapid and sensitive method for the quantitation of microgram quantities of protein utilizing the principle of protein-dye binding. *Anal Biochem.* **72**, 248-254.

Broliden, K., Tolfvenstam, T., Norbeck, O. (2006) Clinical aspects of parvovirus B19 infection. *J Intern Med.* **260**, 285-304.

Brown, K. E., Anderson, S. M., Young, N. S. (1993) Erythrocyte P antigen: cellular receptor for B19 parvovirus. *Science* **262**, 114-117.

Carlson, J., Afanasiev, B., and Suchman, E. (2000) Densoviruses as transducing vectors for insects. In "Insect Transgenesis: Methods and Applications" (E. Handler and A. James, eds.), pp. 139–159. CRC Press, Boca Raton.

Carlson, J., Suchman, E. Buchatsky, L. (2006) Densoviruses for control and genetic manipulation of mosquitoes. *Adv Virus Res* **68**, 361-392.

Castagna, M., Shayakul, C., Trotti, D., Sacchi, V. F., Harvey, W. R., Hediger, M. A. (1998) Cloning and characterization of a potassium-coupled amino acid transporter. *Proc Natl Acad Sci U S A* **95**, 5395-5400.

Cotmore, S. F., Tattersall, P. (2007) Parvoviral host range and cell entry mechanisms. *Adv Virus Res.* **70**, 183-232.

Daimon, T., Katsuma, S., Iwanaga, M., Kang, W., Shimada, T. (2005) The BmChi-h gene, a bacterial-type chitinase gene of *Bombyx mori*, encodes a functional exochitinase that plays a role in the chitin degradation during the molting process. *Insect Biochem Mol Biol.* **35**, 1112-1123.

Doira, H. (1992) Genetical Stocks and Mutations of Bombyx mori. In: Important Genetic Resources (ed.: H. Doira), pp. 1-73. Silkworm Genetic Division, Institute of Genetic Resources, Faculty of Agriculture, Kyushu University, Fukuoka, Japan.

Eguchi, R., Ninaki, O., Hara, W. (1991) Genetical analysis on the nonsusceptibility to densonucleosis virus in the silkworm, Bombyx mori. *J. Seric. Sci. Jpn.* **60**, 384-389. (In Japanese with English summary).

Eguchi, R., Nagayasu, K., Ninaki, O., Hara, W. (2007) Genetic analysis on the dominant non-susceptibility to densonucleosis virus type 1 in the silkworm, Bombyx mori. *SANSHI-KONTYU BIOTEC*, 159-163.

Fediere, G. (2000) Molecular biology of Densovirinae. *Contrib Microbiol* **4**, 1-11.

Fauquet C. M., Mayo M. A., Maniloff J., Desselberger U., and Ball L. A. (eds.) (2005) Virus taxonomy. VIIIth report of the international committee on taxonomy of viruses. Academic Press pp1162.

Feldman, D. H., Harvey, W. R., Stevens, B. R. (2000) A novel electrogenic amino acid transporter is activated by K^+ or Na^+, is alkaline pH-dependent, and is Cl^--independent. *J Biol Chem* **275**, 24518-24526.

Furuta Y (1994) Susceptibility of Indian races of the silkworm, *Bombyx mori*, to the nuclear polyhedrosis virus and densonucleosis viruses. *Acta Seric Entomol* **8**, 1-10.

Furuta Y (1995) Susceptibility of the races of the silkworm, *Bombyx mori*, preserved in NISES to the nuclear polyhedrosis virus and densonucleosis viruses. *Bull Natl Inst Seric Entomol Sci* **15**, 119-145.

Goldsmith, M. R. (1995) Genetics of the silkworm: revisiting an ancient model system. In: Molecular Model Systems in the Lepidoptera. (eds.: M. R. Goldsmith, and A. S. Wilkins), pp. 21-76. Cambridge Univ. Press, New York.

Goldsmith MR, Shimada T, Abe H (2005) The genetics and genomics of the silkworm, *Bombyx mori*. *Annu Rev Entomol* **50**: 71-100.

Gopalapillai, R., Kadono-Okuda, K., Tsuchida, K., Yamamoto, K., Nohata, J., Ajimura, M., Mita, K., 2006. Lipophorin receptor of Bombyx mori: cDNA cloning, genomic structure, alternative splicing, and isolation of a new isoform. *J Lipid Res.* **47**, 1005-1013.

Jousset, F. X., Barreau, C., Boublik, Y., Cornet, M. (1993) A parvo-like virus persistently infecting a C6/36 clone of Aedes albopictus mosquito cell line and pathogenic for Aedes aegypti larvae. *Virus Res.* **29**, 99-114.

Kadono-Okuda K., Kosegawa, E., Mase, K., Hara, H. (2002) Linkage analysis of maternal EST cDNA clones covering all twenty-eight chromosomes in the silkworm, Bombyx mori. *Insect Mol Biol* **11**, 443-451.

Kaufmann, B., Simpson, A. A., Rossmann, M. G. (2004) The structure of human parvovirus B19. *Proc Natl Acad Sci U S A.* **101**, 11628-11633.

Katsuma S, Mita K, Shimada T. (2007) ERK- and JNK-dependent signaling pathways contribute to Bombyx mori nucleopolyhedrovirus infection. *J Virol.* **81**, 13700-13709.

Kawase, S., Kurstak, E. (1991) in *Viruses of Invertebrates*, ed Kurstak E (Marcel Dekker, New York) pp315-343.

Koike, Y., Mita, K., Suzuki, M. G., Maeda, S., Abe, H., Osoegawa, K., deJong, P. J., Shimada, T. (2003) Genomic sequence of a 320-kb segment of the Z chromosome of *Bombyx mori* containing a *kettin* ortholog. *Mol Genet Genomics* **269**, 137-149.

Li, M., Guo, Q., Hou, C., Miao, X., Xu, A., Guo, X., Huang, Y. (2006) Linkage and mapping analyses of the densonucleosis non-susceptible gene *nsd-Z* in the silkworm *Bombyx mori* using SSR markers. *Genome* **49**, 397-402.

Li, Y., Jousset, F. X., Giraud, C., Rolling, F., Quiot, J. M., Bergoin, M. (1995) A titration procedure of the Junonia coenia densovirus and quantitation of transfection by its cloned genomic DNA in four lepidopteran cell lines. *J Virol Methods* **57**, 47-60.

Mackrell, A. J., N. W. Soong, C. M. Curtis, and W. F. Anderson. (1996) Identification of a subdomain in the Moloney murine leukemia virus envelope protein involved in receptor binding. *J. Virol.* **70**, 1768-1774.

Meng, Y., Katsuma, S., Mita, M., Shimada, T. (2009) Abnormal red body coloration of the silkworm, *Bombyx mori*, is caused by a mutation in a novel kynureninase. *Genes to Cells* **14**, 129-140.

Mita, K., Kasahara, M., Sasaki, S., Nagayasu, Y., Yamada, T., Kanamori, H., Namiki, N., Kitagawa, M., Yamashita, H., Yasukochi, Y., Kadono-Okuda, K., Yamamoto, K., Ajimura, M., Ravikumar, G., Simomura, M., Nagamura, Y., Shin-I, T., Abe, H., Shimada, T., Morishita, S., Sasaki, T. (2004) The genome sequence of silkworm, *Bombyx mori*. *DNA Res* **11**, 27-35.

Munakata, Y., Saito-Ito, T., Kumura-Ishii, K., Huang, J., Kodera, T., Ishii, T., Hirabayashi, Y., Koyanagi, Y., Sasaki, T. (2005) Ku80 autoantigen as a cellular coreceptor for human parvovirus B19 infection. *Blood*. **106**, 3449-3456.

Nguu, E. K., Kadono-Okuda, K., Mase, K., Kosegawa, E., Hara, W. (2005) Molecular linkage map for the silkworm, *Bombyx mori*, based on restriction fragment length polymorphism of cDNA clones. *J. Insect Biotechnol. Seriocol* **74**, 5-13.

Ogoyi, D. O., Kadono-Okuda, K., Eguchi, R., Furuta, Y., Hara, W., Nguu, E. K., Nagayasu, K. (2003) Linkage and mapping analysis of a non-susceptibility gene to densovirus (*nsd-2*) in the silkworm, *Bombyx mori*. *Insect Mol Biol* **12**, 117-124.

Palermo, L. M., Hueffer, K., Parrish, C. R. (2003) Residues in the apical domain of the feline and canine transferrin receptors control host-specific binding and cell infection of canine and feline parvoviruses. *J Virol* **77**, 8915-8923.

Parker, J. S. and Perrish, C. R. (2000) Cellular uptake and infection by canine parvovirus involves rapid dynamin-regulated clathrin-mediated endocytosis, followed by slower intracellular trafficking. *J Virol* **74**, 1919-1930.

Qian, Z., Donald, R., Wang, H., Chen, Q., and Albritton, L. M. (2003) Identification of a

Critical Basic Residue on the Ecotropic Murine Leukemia Virus Receptor. *J. Virol.* **77**, 8596-8601.

Qin, J. & Yi, W. Z. (1996) Genetic linkage analysis of *nsd-Z*, the nonsusceptibility gene of *Bombyx mori* to the Zhenjiang (China) strain densonucleosis virus. *Sericologia* **36**, 241-244.

Seki, H., and Iwashita, Y. (1983) Histopathological features and pathogenicity of a densonucleosis virus of the silkworm, Bombyx mori, isolated from sericultural farms in Yamanashi prefecture. *J. Seric. Sci. Jpn.* **52**, 400-405. (In Japanese with English summary).

Seki, H. (1984) Mode of inheritance of the resistance to the infection with the densonucleosis virus (Yamanashi isolate) in the silkworm, Bombyx mori. *J. Seric. Sci. Jpn.* **53**, 472-475. (In Japanese with English summary).

Shimizu, T. (1975) Pathogenicity of an infectious flacherie virus of the silkworm, Bombyx mori, obtained from sericultural farms in the suburbs of Ina city. *J. Seric. Sci. Jpn.* **44**, 45-48. (In Japanese).

Shirk, P. D., Bossin, H., Furlong, R. B., Gillett, J. L. (2007) Regulation of *Junonia coenia* densovirus P9 promoter expression. *Insect Mol Biol.* **16**, 623-33.

Solheim, B. G., Rollag, H., Svennevig, J. L., Arafa, O., Fosse, E., Bergerud, U. (2000) Viral safety of solvent/detergent-treated plasma. *Transfusion.* **40**, 84-90.

Suchman, E. L., Kononko, A., Plake, E., Doehling, M., Kleker, B., Black, W. C., Buchatsky, L., and Carlson, J. (2006) Effects of AeDNV infection on Aedes aegypti (L.) lifespan and reproduction. *Biol. Control.* **39**, 465-473.

Sundin, M., Lindblom, A., Orvell, C., Barrett, A. J., Sundberg, B., Watz, E., Wikman, A., Broliden, K., Le, Blanc, K. (2008) Persistence of human parvovirus B19 in

multipotent mesenchymal stromal cells expressing the erythrocyte P antigen: implications for transplantation. *Biol Blood Marrow Transplant.* **14**, 1172-1179

Tattersall, P., Bergoin, M., Bloom, M. E., Brown, K. E., Linden, R. M., Muzyczka, N., Parrish, C. R., and Tijssen, P. (2005). Parvoviridae. In ‘‘Virus Taxonomy, VIIIth Report of the ICTV’’ (C. M. Fauquet, M. A. Mayo, J. Maniloff, U. Desselberger, and L. A. Ball, eds.), pp. 353–369. Elsevier/Academic Press, London.

Tamura, T., Thibert, C., Royer, C., Kanda, T., Abraham, E., Kamba, M., Komoto, N., Thomas, J. L., Mauchamp, B., Chavancy, G., Shirk, P., Fraser, M., Prudhomme, J. C., Couble, P. (2000) Germline transformation of the silkworm *Bombyx mori* L. using a *piggyBac* transposon-derived vector. *Nat Biotechnol* **18**, 81-84.

Tijssen, P., and Bergoin, M. (1995) Densonucleosis viruses constitute an increasingly diversified subfamily among the parvoviruses. Semin. *Virol*. **6**, 347-355.

Wang, Y. J., Yao, Q., Chen, K. P., Wang, Y., Lu, J., Han. X. (2007) Characterization of the genome structure of Bombyx mori densovirus (China isolate). *Virus Genes* **35**, 103-108.

Ward, T. W., Kimmick, M. W., Afanasiev, B. N., Carlson, J. O. (2001) Characterization of the structural gene promoter of *Aedes aegypti* densovirus. *J Virol*. **75**, 1325-1331.

Watanabe, H., Maeda, S., Matsui, M., and Shimizu, T. (1976) Histopathology of the midgut epithelium of the silkworm, *Bombyx mori*, infected with a newly-isolated virus from the flacherie-diseased larvae. *J. Seric. Sci. Jpn*. **45**, 29-34. (In Japanese with English summary).

Watanabe, H., and Maeda, S. (1978) Genetic resistance to peroral infection with a densonucleosis virus in the silkworm, *Bombyx mori*. *J. Seric. Sci. Jpn*. **47**, 209-214. (In Japanese with English summary).

Watanabe, H. and Maeda, S. (1981) Genetically determined nonsusceptibility of the silkworm, *Bombyx mori*, to infection with a densonucleosis virus (densovirus). *J. Invertebr. Pathol.* **38**, 370-373.

Watanabe, H., Kawase, S., Shimizu, T., and Seki, H. (1986) Difference in serological characteristics of densonucleosis viruses in the silkworm, *Bombyx mori*. *J. Seric. Sci. Jpn*. **55**, 75-76. (In Japanese).

Watanabe, H. (2002) Genetic resistance of the silkworm, *Bombyx mori* to viral diseases, *Curr. Sci.* **83**. 439–446.

Weigel-Kelley, K. A., Yoder, M. C., Srivastava, A. (2003) Alpha5beta1 integrin as a cellular coreceptor for human parvovirus B19: requirement of functional activation of beta1 integrin for viral entry. *Blood.* **102**, 3927-3933.

Xia, Q., Zhou, Z., Lu, C., Cheng, D., Dai, F., Li, B., Zhao, P., Zha, X., Cheng, T., Chai, C., Pan, G., Xu, J., Liu, C., Lin, Y., Qian, J., Hou, Y., Wu, Z., Li, G., Pan, M., Li, C., Shen, Y., Lan, X., Yuan, L., Li, T., Xu, H., Yang, G., Wan, Y., Zhu, Y., Yu, M., Shen, W., Wu, D., Xiang, Z., Yu, J., Wang, J., Li, R., Shi, J., Li, H., Li, G., Su, J., Wang, X., Li, G., Zhang, Z., Wu, Q., Li, J., Zhang, Q., Wei, N., Xu, J., Sun, H., Dong, L., Liu, D., Zhao, S., Zhao, X., Meng, Q., Lan, F., Huang, X., Li, Y., Fang, L., Li, C., Li, D., Sun, Y., Zhang, Z., Yang, Z., Huang, Y., Xi, Y., Qi, Q., He, D., Huang, H., Zhang, X., Wang, Z., Li, W., Cao, Y., Yu, Y., Yu, H., Li, J., Ye, J., Chen, H., Zhou, Y., Liu, B., Wang, J., Ye, J., Ji, H., Li, S., Ni, P., Zhang, J., Zhang, Y., Zheng, H., Mao, B., Wang, W., Ye, C., Li, S., Wang, J., Wong, G. K., Yang, H.; Biology Analysis Group. (2004) A draft sequence for the genome of the domesticated silkworm (*Bombyx mori*). *Science* **306**, 1937-1940.

Yamamoto, K., Narukawa, J., Kadono-Okuda, K., Nohata, J., Sasanuma, M., Suetsugu,

Y., Banno, Y., Fujii, H., Goldsmith, M. R., Mita, K. (2006) Construction of a single nucleotide polymorphism linkage map for the silkworm, *Bombyx mori*, based on bacterial artificial chromosome end sequences. *Genetics* **173**, 151-161.

Yamamoto, K., Nohata, J., Kadono-Okuda, K., Narukawa, J., Sasanuma, M., Sasanuma, S., Minami, H., Shimomura, M., Suetsugu, Y., Osoegawa, K., de Jong, P. J., Goldsmith, M. R., Mita, K. (2008) A BAC-based integrated linkage map of the silkworm Bobmyx mori. *Genome Biol*. **9**, R21.

Yoshimoto, T., Yoshimoto, E., Meruelo, D. (1991) Molecular cloning and characterization of a novel human gene homologous to the murine ecotropic retroviral receptor. *Virology* **185**, 10-17.